Supporting Information

Unveiling the Urease Like Intrinsic Catalytic Activities of Two Dinuclear Nickel Complexes towards *in-situ* Syntheses of Aminocyanopyridines

Bidyut Kumar Kundu,[a] Pragti,[a] Soumen Biswas,[a, b] Abhijit Mondal,[c] Shyamalava Mazumdar,[c] Shaikh M. Mobin,[a] Suman Mukhopadhyay[a, d, *]

[a] Discipline of Chemistry, School of Basic Sciences, Indian Institute of Technology Indore, Simrol, Khandwa Road, Indore 453552, India

[b] Department of Chemistry, School of Applied Sciences, Centurion University of Technology and Management, Bhubaneswar-752050, Odisha, India

[c] Department of Chemistry, Research Institute for Natural Sciences and Center for New Directions in Organic Synthesis (CNOS), Hanyang University, 222 Wangsimni-ro, Seongdong-gu, Seoul 04763, Korea

[d] Department of Chemistry, Tata Institute of Fundamental Research, Homi Bhabha Road, Colaba, Mumbai 400 005, India

[e] Discipline of Biosciences and Biomedical Engineering, School of Basic Sciences, Indian Institute of Technology Indore, Khandwa Road, Simrol, Indore 453552, India

***** E-mail: suman@iiti.ac.in; Fax: +91 731 2361; Tel: +91 731 2438 735

Table of contents

Abbreviations

Entry	*Significance*	*Entry*	*Significance*
HL^1	2,4-dimethyl-6-{[(2'-dimethyl aminoethyl) methylamino]methyl}-phenol	**XRD**	X-ray diffraction
HL^2	2,4-dichloro-6-{[(2'-dimethyl aminoethyl) methylamino]methyl}-phenol	**equiv**	Equivalent
NMR	Nuclear magnetic resonance	**UV-Vis**	Ultraviolet-Visible
ESI-MS	Electrospray ionisation mass spectrometry	**T**	Temperature
FTIR	Fourier transformed infra-red	**sym/ sy**	Symmetric
HeLa	Human cervical cancer cell lines	**r.t.**	Room temperature
λ_{ex}/ λ_{em}	Excitation/ emission wavelength	**GC**	Gas chromatography
λ_{max}	Wavelength maximum	**h/ min**	hour/ minute

Section S1. Experimental Section

General Remarks for Characterization: ^{1}H and ^{13}C NMR spectroscopy were conducted on an AVANCE III 400 Ascend Bruker BioSpin instrument at room temperature (r.t). Infrared (FTIR) spectra (range: 4000 to 500 cm^{-1}) was record by BRUKER TENSOR 27 machine. Elemental analyses (C, H, N and S content) were performed with a ThermoFlash 2000 elemental analyzer. Mass spectrometric analyses were carried out on Bruker-Daltonics, MicroTOF-Q II mass spectrometer. Spectrophotometric measurements for absorption study were done using a quartz cuvette with a path length of 1 cm on a Varian UV/Vis spectrophotometer (Model: Cary 100). Thermogravimetric analysis (TGA) was conducted on a "METTLER TOLEDO" TGA/DSC 1 Module with a heating rate of 10 °C min^{-1} with a sensitivity of 10 mg in the temperature range of 0-800 °C and the TGA data was analyzed by "STAR^{e} Software" under a static N_2 atmosphere. Stopped-flow spectrometery was carried out by a BioLogic Sciences Instruments (Seyssinet-Pariset, France) SFM4000 apparatus. The cyclization products throughout catalysis were quantitatively identified by GC experiments using GC-MS QP 2010 Ultra mass spectrometer from Shimadzu Analytical India Pvt. Ltd.

Section S2. X-ray crystallography

Single crystal X-ray structural studies of Mannich base ligand **(HL^2)**, complex **1** and complex **2** were performed on a CCD Agilent Technologies (Oxford Diffraction) SUPER NOVA diffractometer, among which **HL^2** has reported with CCDC **1882115**.[1] Data for both the compounds were collected at 150-293 K using a graphite-monochromated MoKα radiation (λ_α = 0.71073 Å). The strategy for the data collection was evaluated by using the CrysAlisPro CCD software.[2] The data were collected by the standard 'phi-omega scan techniques and were scaled and reduced using CrysAlisPro RED software. The structures were solved by direct methods using SHELXS-97 and refined by full matrix least-squares with SHELXL-97, refining on F^2.[3] The positions of all the atoms were obtained by direct methods. All non-hydrogen atoms were refined anisotropically. The remaining hydrogen atoms were placed in geometrically constrained positions and refined with isotropic temperature factors, generally 1.2U_{eq} of their parent atoms. The crystal and refinement data are summarized in Table 1 and corresponding bond lengths, bond angles and other crystallographic details are summarized in Table S2-S7.

Section S3. Materials and methods

S3.1. Hirshfeld surface analysis

In addition, Hirshfeld surface analysis (Figure S8) has been carried out to corroborate the possible supramolecular interactions of the synthesized complexes as described in Figure S7. The molecular Hirshfeld surface[4] is formed based on the electron distribution of a molecule and has been determined as the sum of spherical atom electron densities.[5] For a given crystal structure and set of spherical atomic electron densities, the Hirshfeld surface is unique.[6] Equation (1), which is based on both d_e and d_i, and the van der Walls radii of the atom give the normalized contact distance (d_{norm}), where d_e is the distance from the point to the nearest nucleus external to the surface, and d_i is the distance to the nearest nucleus internal to the surface. The 2D fingerprint plot provides a summary of intermolecular contacts in the crystal.[6-7] The Hirshfeld surfaces presented here were generated using Crystal Explorer 3.1.[8] The symmetrically generated counterpart of the structures was not taken into account in Hirshfeld surface calculations.[9]

$$d_{norm} = \frac{d_i - r_i^{vdw}}{r_i^{vdw}} + \frac{d_e - r_e^{vdw}}{r_e^{vdw}} \ldots \qquad \ldots (1)$$

S3.2. Ammonia Assay

Ammonia was analyzed by using an indophenol assay procedure as per earlier report.[10]

Reagents Solutions: NH_3 containing H_3BO_3, Cl_2-H_2O, 8% PhOH in H_2O, 3N NaOH

Attention: *Ammonia (NH_3) free water should be used throughout the assay. These reagents can be stored in a refrigerator for about 1 month without decomposition. Though, here the experiments have been carried out with freshly prepared solution!*

- Preparation of Solutions: Step I- Preparation of NH_3-H_3BO_3 solution

Known volume (< 250 mL) of water was taken into the collection chamber and proper apparatus was set-up followed by the maintenance of optimized reaction conditions for ammonia production. After urea hydrolysis, the NH_3 mixed water solution was taken in a conical flask and boric acid (13.88 g) was added into it. The volume was made up by water up to 250 mL to have the stock solution followed by the transfer 25 mL solution in a 50 mL of volumetric flask.

- Step II- Preparation of Cl_2-H_2O

5% alkaline hypochlorite (NaOCl, 180 mL) was added to 12M of hydrochloride (HCl, 20 mL) acid, which was poured into 800 mL water (H_2O) to produce 0.12 mol of molecular chlorine solution.

Color development procedure: After filled by H_3BO_3-NH_3 solution, 5 mL of Cl_2-H_2O and 5 mL of 8% phenol solutions were added in each 50 mL volumetric flask. Further the volumetric flasks were heated in the hot plates at 100 °C for 3 min and cooled down rapidly. Add 5 mL of 3M NaOH and dilute to volume. The blue color developed fully from faint yellow within 5 min (See the following reaction). Read the absorbance of the blue solutions in a 1 cm cuvette at 629 nm against a reagent blank. When the complexes and substrates themselves were assayed, no absorbance at 629 nm was observed. The concentrations of unknown ammonia solutions have been obtained from the standard calibration curve (Figure S15).

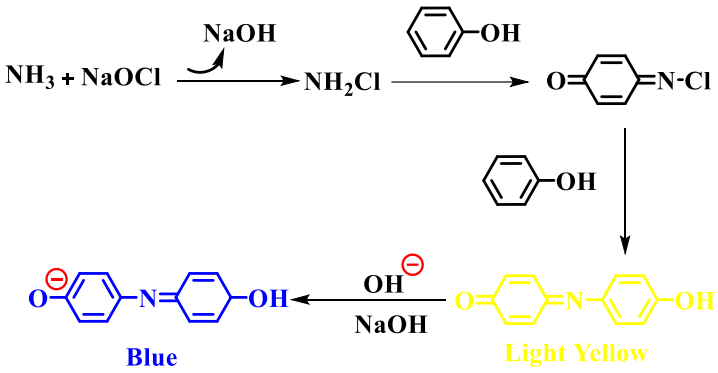

A calibration curve was obtained by adding aliquots of standard NH_3 solution (30-330 ppm), which have been prepared as abovementioned color developing method. Only standard NH_3 solution has been used instead of Step-I.

- Step III- Preparation of standard NH_3 solution for calibration

A stock solution was prepared containing 1000 ppm of NH_3 by dissolving 3.145 g of dry NH_4Cl in 1 L of ammonia-free water.

Quantitative measurement of ammonia[11]

Determination of the concentration of unknown samples:

O.D value of unknown samples are 0.1288 and 0.1395 for dinickel mimetics **1** and **2**, respectively (from the reaction between 2 mmol urea and 0.02 mmol of each complex at 59 °C in aqueous medium for 2 h). Each measurement replicates for three times and average value has been considered for final quantitative evaluation.

As, from the Lambert- Beer's law; $A = \text{Ɛ}cl$ … … (i)

And from the linear equation; $Y = mX + C$ … … (ii)

Where, A = Absorbance or optical density (O.D), Ɛ = Molar extinction coefficient, c = Concentration, l = Path length of the cell (here 1 cm), m = Slope and C = Intercept

Which means at C = 0, the equation (ii) becomes to $Y = mX$ … … (iii)

Comparing equations (i) and (iii), we get; m = Ɛ

From the standard calibration curve as discussed above, we have

Slope (Ɛ) = m = 0.0026 (by fixing the intercept, C = 0)

Now, for the determination of unknown sample concentration;

By using equation (i):

A = Ɛcl

or, 0.1288 = 0.0026 × c × 1 (considering dinickel mimetic **1**)

or, c = 49.54 ppm

Now, 1 ppm = 1 mg/L

So, 49.54 ppm = 49.54 mg/L

Now, to calculate the mole of NH_3 production in the reaction is:

So, molarity = 49.54 (mg/L) / 17.031 (g/mol) = 49.54/(17.031*1000) (mol/L) = 49.54/17.031 (mmol/L) = 2.9088 (mmol/L)

Similarly, for dinickel mimetic **2** the value is 53.65 ppm ≡ 3.15036 (mmol/L).

Section S4. Figures

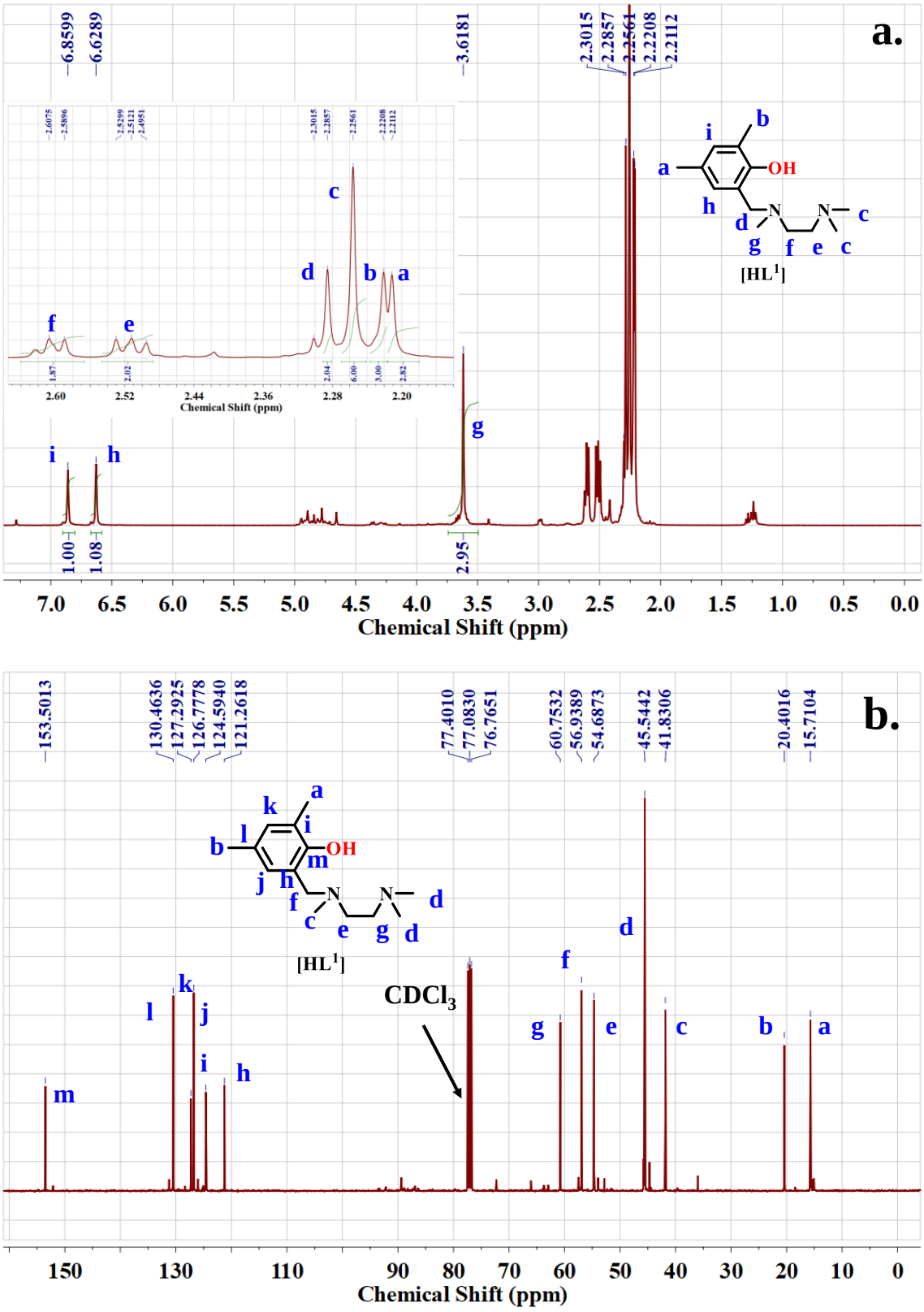

Figure S1. (a) ^{1}H (400.13 MHz, 298K, $CDCl_3$) and (b) ^{13}C (100.61 MHz, 298K, $CDCl_3$) NMR spectra of **HL^1**. Letters denote the chemical environment for each hydrogen and carbon.

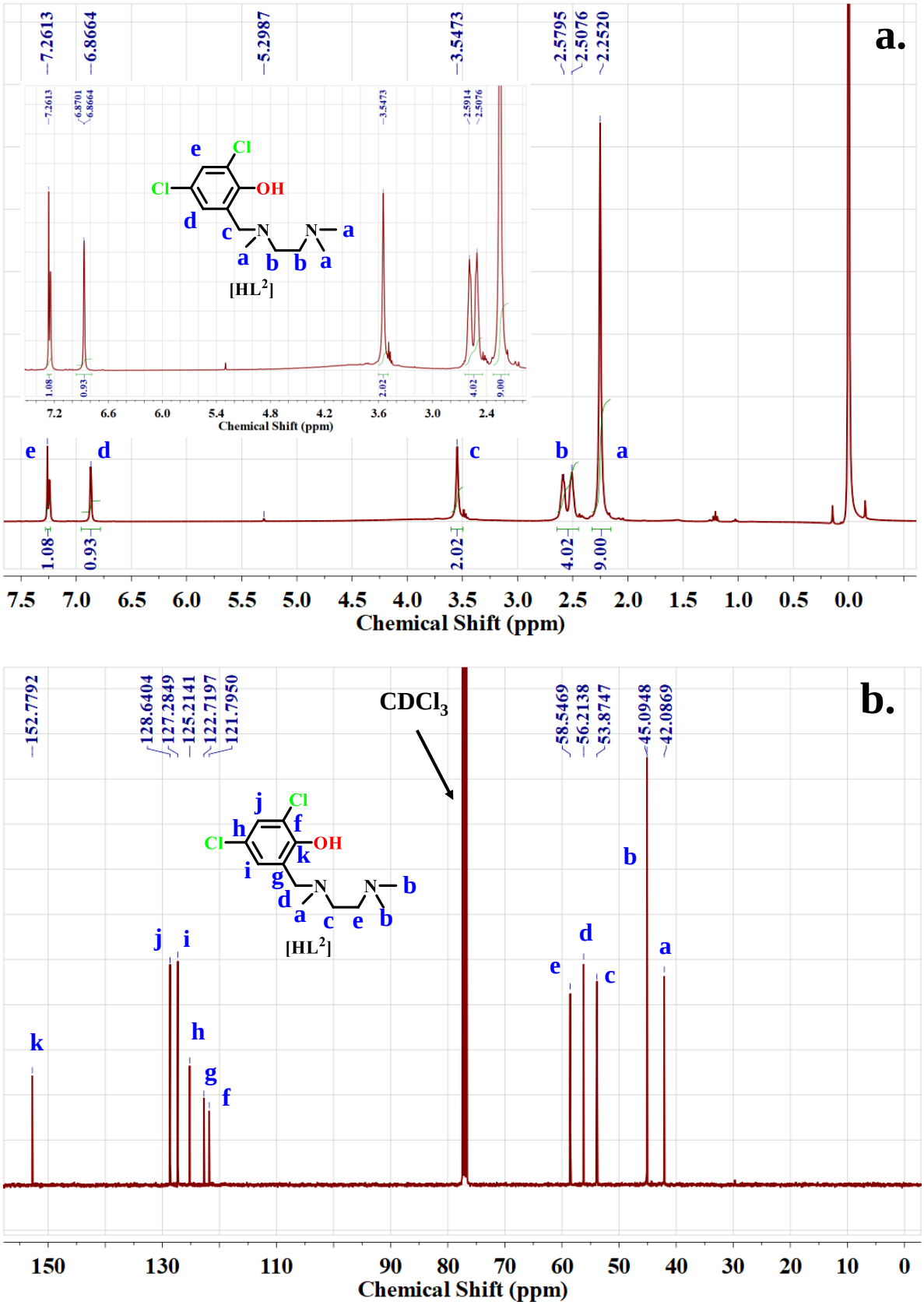

Figure S2. (a) ^{1}H (400.13 MHz, 298K, $CDCl_3$) and (b) ^{13}C (100.61 MHz, 298K, $CDCl_3$) NMR spectra of **HL^2**. Letters denote the chemical environment for each hydrogen and carbon.

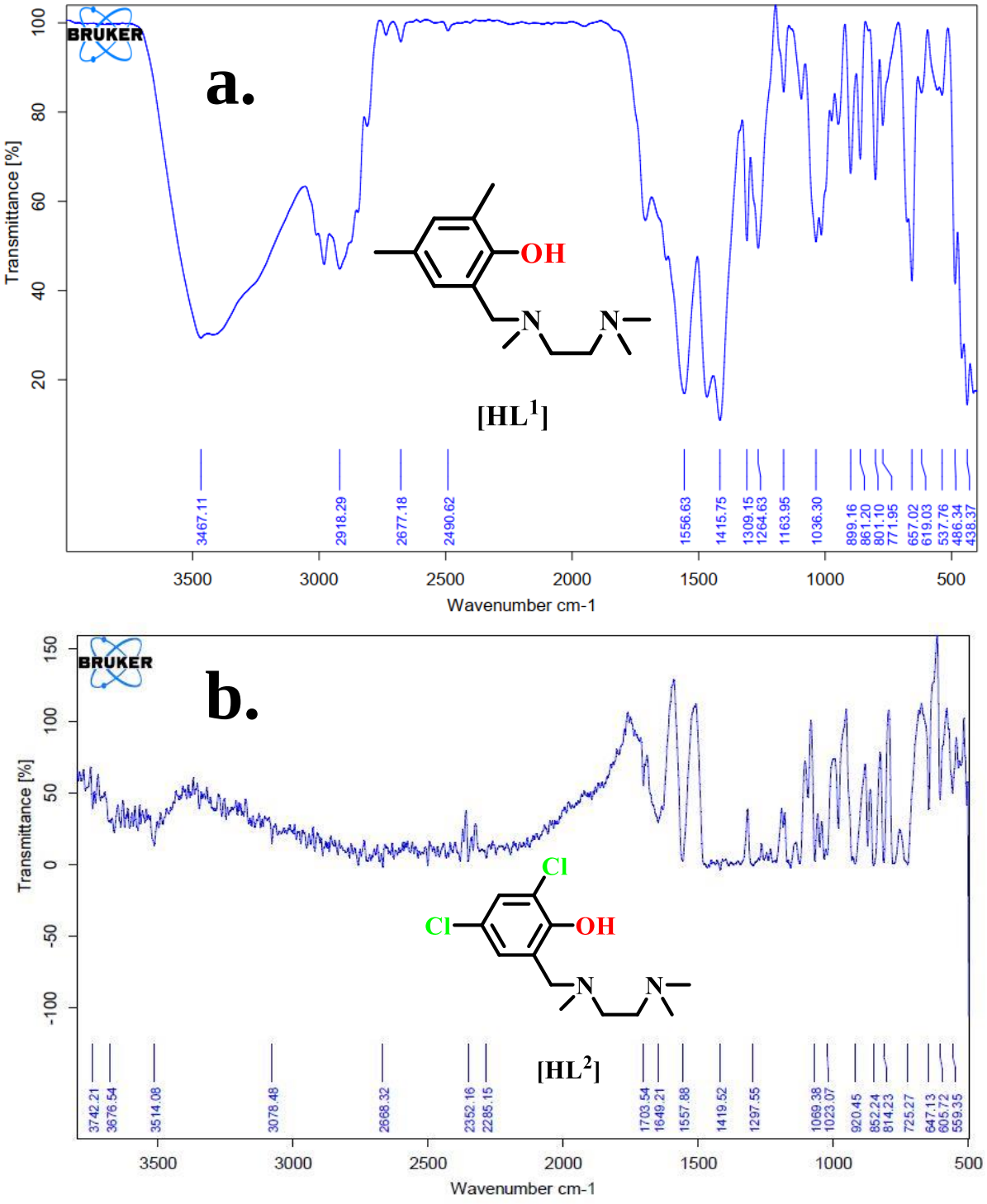

Figure S3. FTIR stretching frequencies (in KBr pallet, solid phase) of Mannich base ligands: (a) **HL^1** and (b) **HL^2**.

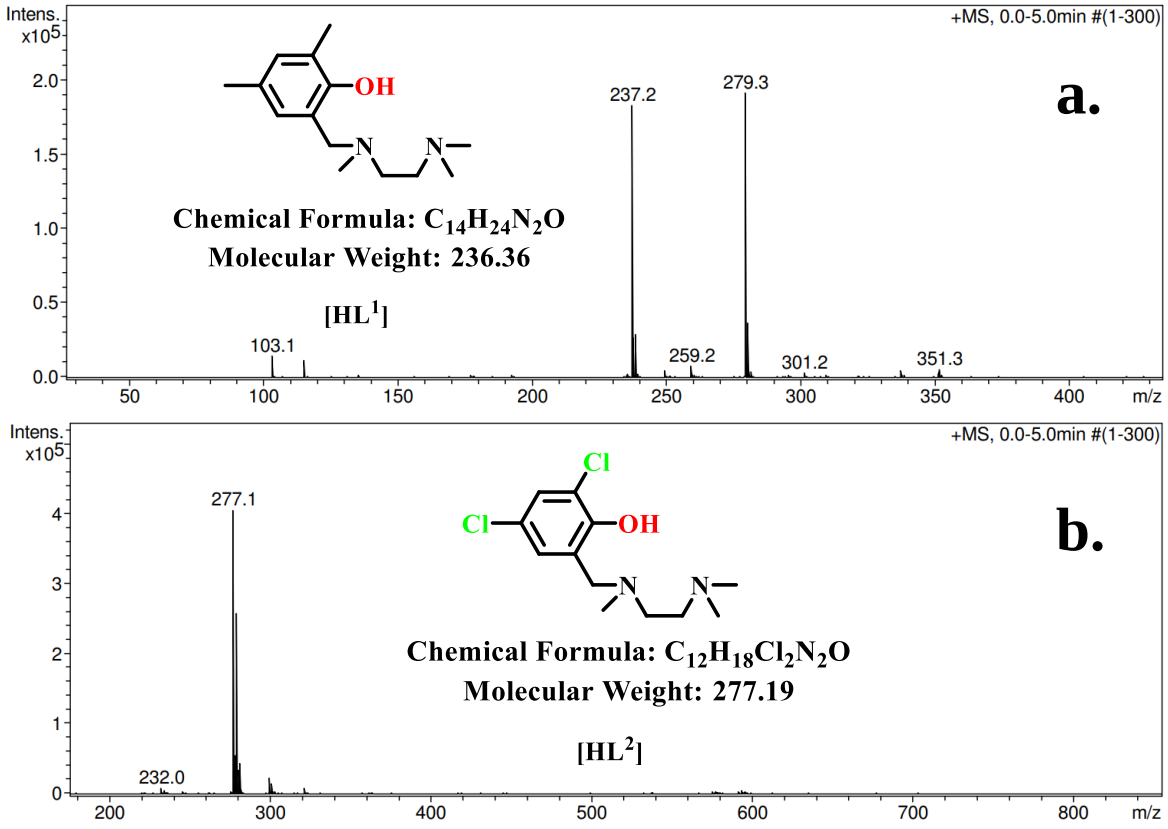

Figure S4. ESI-MS interpretation of Mannich base ligands: (a) **HL**^{1} and (b) **HL**^{2} in HPLC MeOH.

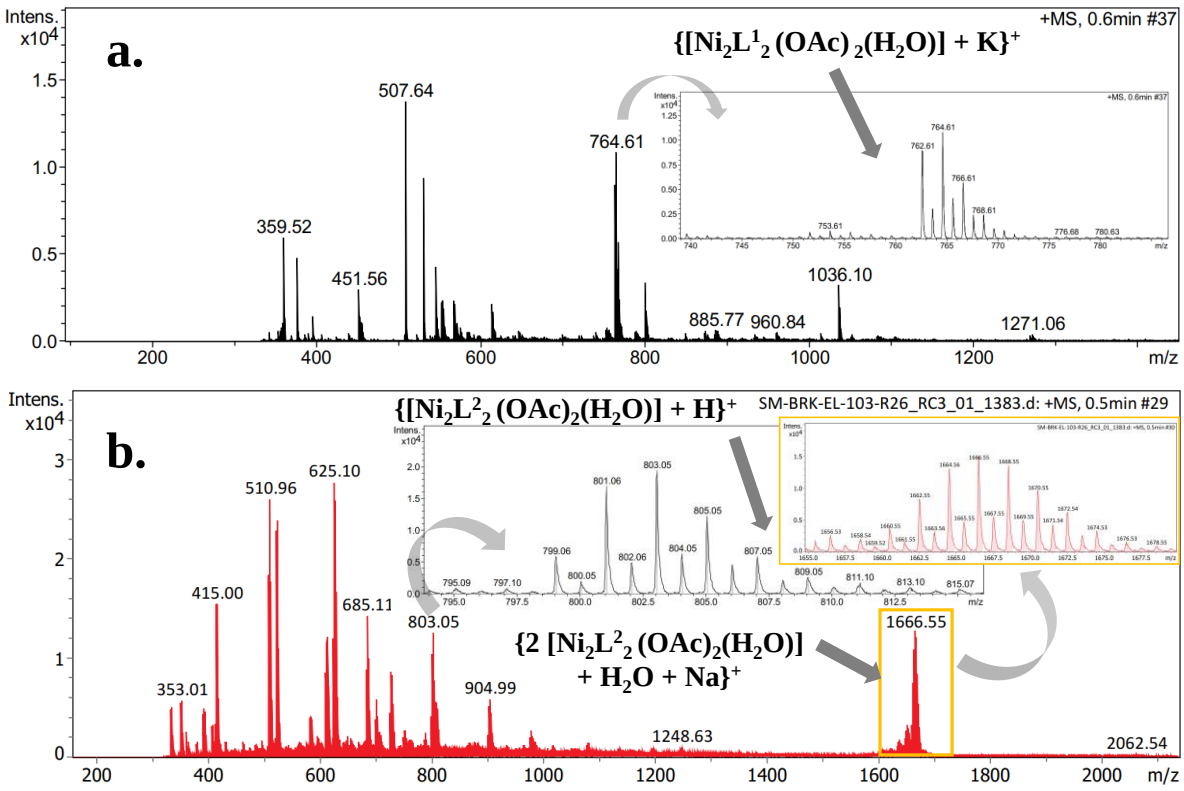

Figure S5. ESI-MS interpretation of dinickel complexes (a) **1** and (b) **2** in HPLC MeOH.

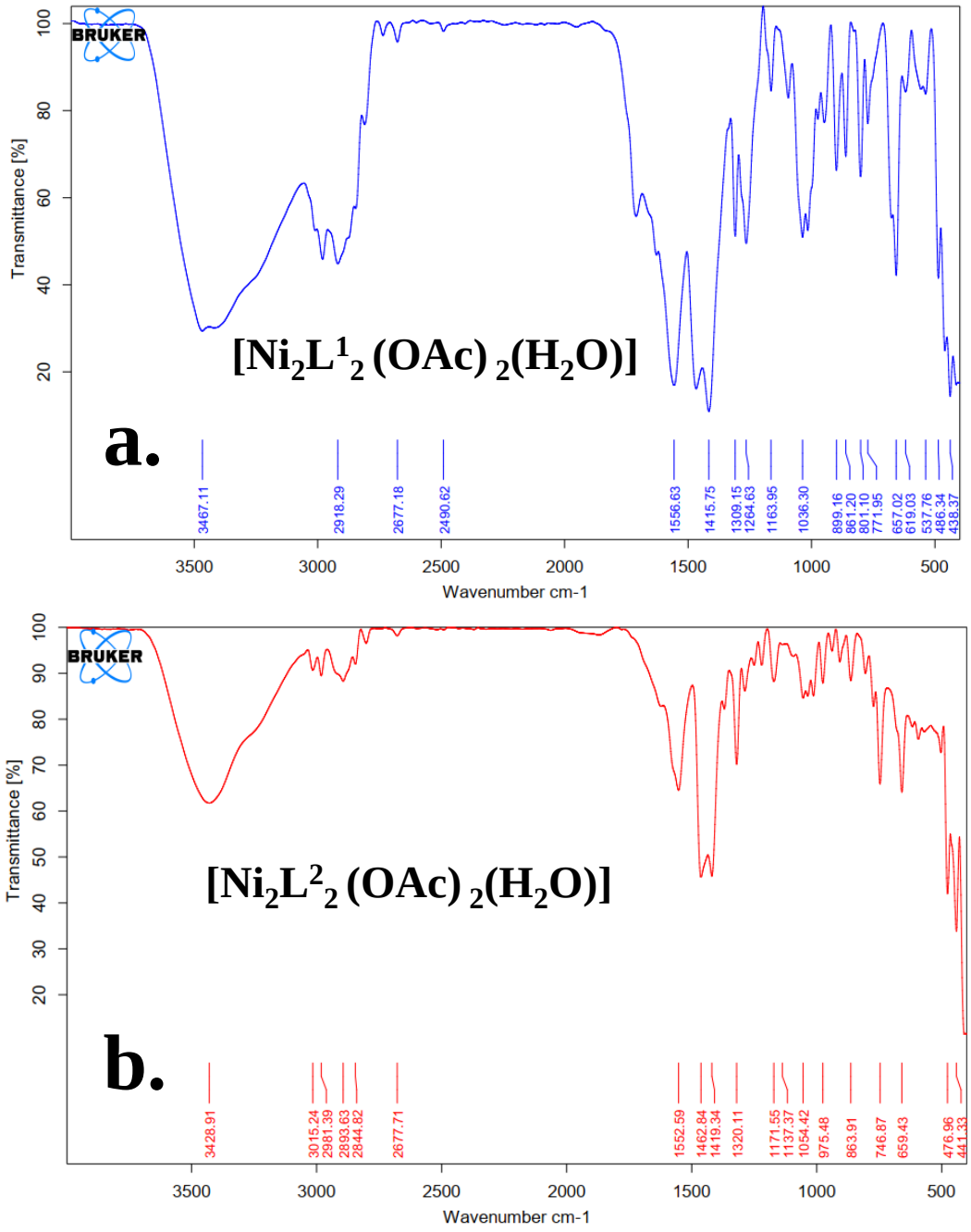

Figure S6. FTIR stretching frequencies (in KBr pallet, solid phase) of dinickel complexes (a) **1** and (b) **2**. The infrared vibrational spectrum shows bands at 861-863 and 438-441 cm^{-1} assigned as υ_{as}(NiONi) and δ(NiONi) respectively and there is also a characteristic band for υ(OH) in the range of 3428-3467 cm^{-1}. Values were compared with published literature.[1, 12]

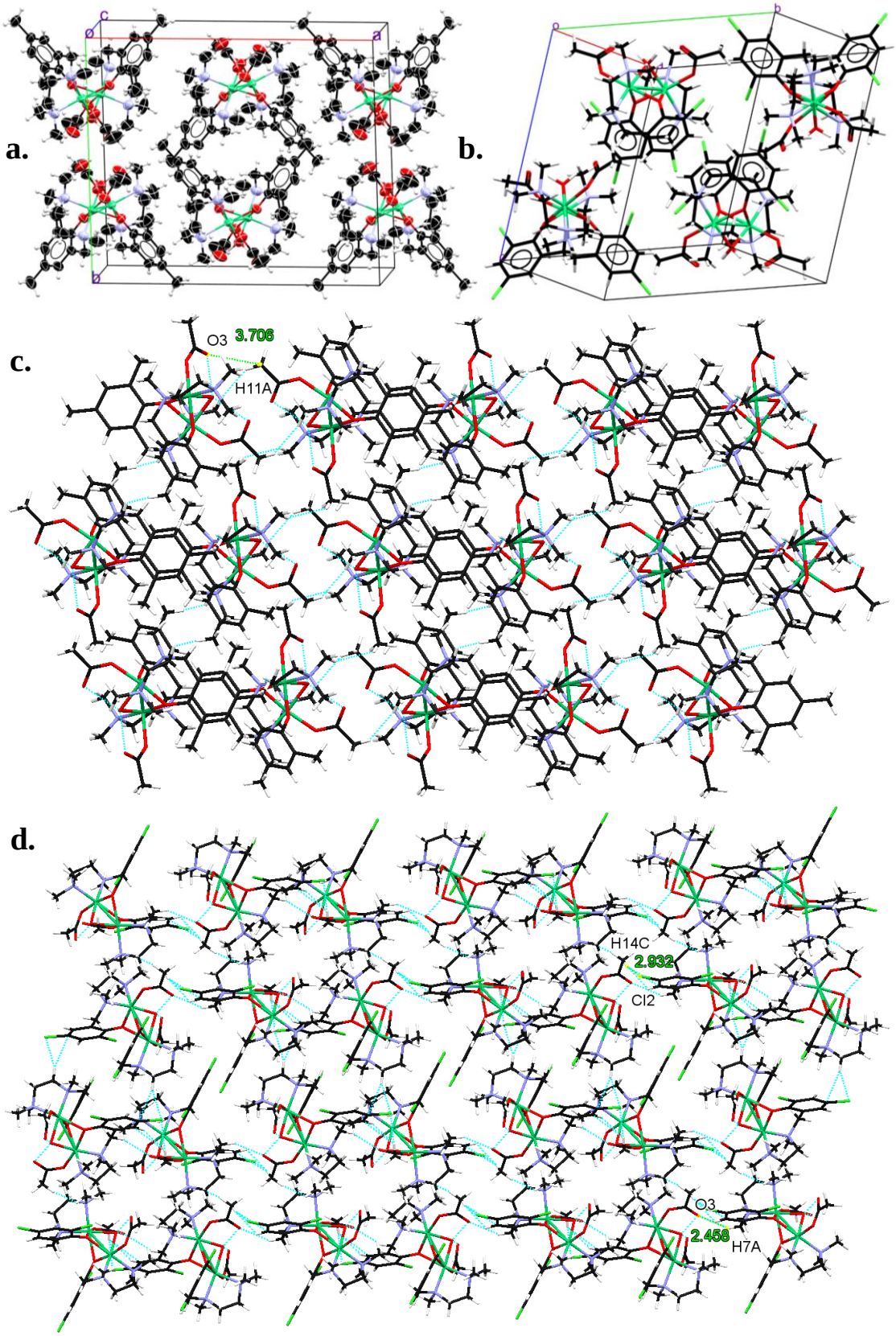

Figure S7. (a) Crystal close packing diagram of complex **1**. (b) Crystal packing diagram of **2**. (c) Supramolecular interactions (hydrogen bonding) *via* O(3)…H(11A) in **1**. (d) Polymer extension of **2** by the help of H-bond through O(3)…H(7A) and Cl(2)…H(14C) contacts.

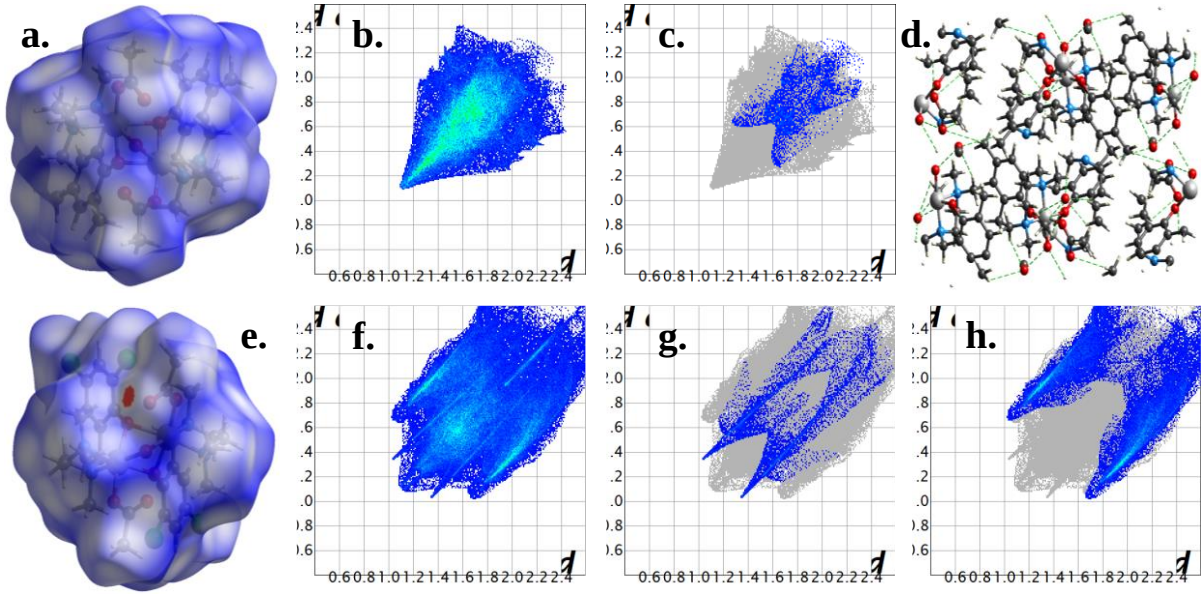

Figure S8. Hirshfeld surfaces mapped with d_{norm} (color scale in between 0.026-1.405 au for both complexes), associated fingerprint plots and some selective supramolecular interaction of the title complexes. Dotted lines in green denote the hydrogen bonds. (a and e) d_{norm} plots of **1** and **2**. (b and f) standard di *vs* de representation of **1** and **2**. (c and g) O...H contacts (7.3% and 6.8% for **1** and **2**, respectively). (d) hydrogen bonding *via* O(3)…H(11A) in complex **1**. (h) Cl...H interactions (27.0%) for complex **2**.

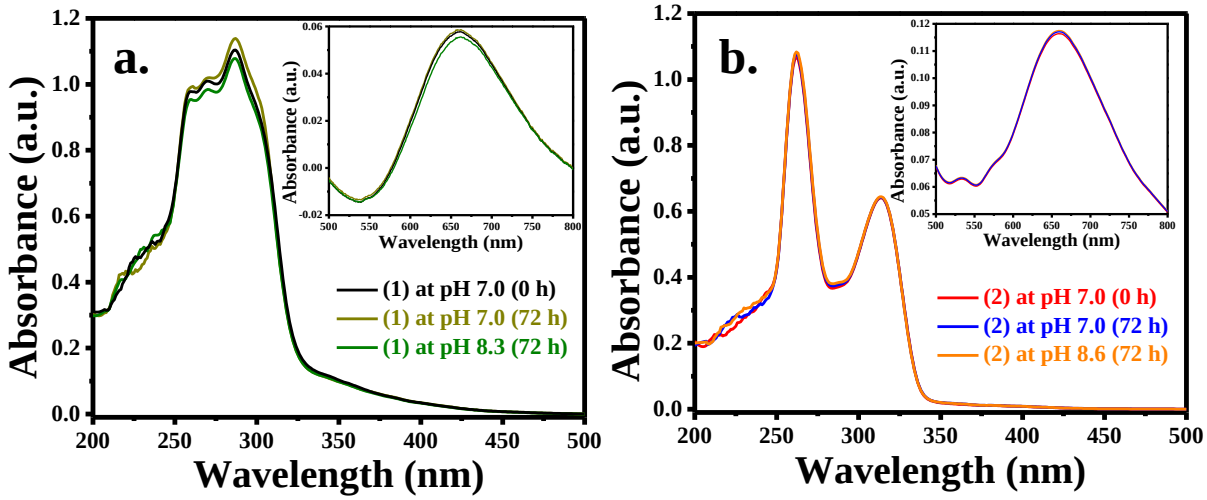

Figure S9. Time and pH dependent stability test through analysing the electronic spectra (in aqueous medium, open atmosphere, 25 °C, in the range of 200-800 nm) of (a) complex **1** having major π→π* band at 287 nm and a d-d transition at 660 nm, (b) complex **2** having major π→π* band at 266 nm, n→π* band at 312 and a d-d transition at 659 nm. The inset shows the absorption spectrum of d-d transitions at 25 °C.

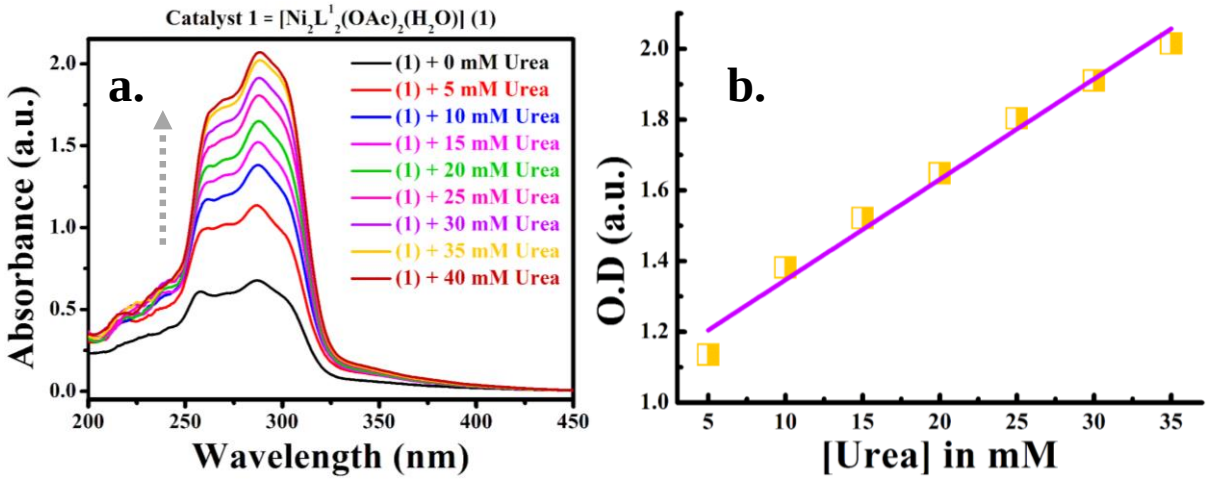

Figure S10. (a) Concentration dependent electronic spectral changes of the complex **1** (0.2 mM) in water under open atmosphere at 25 °C. The spectra were recorded at 40 s intervals. (b) An increment in optical density of **1** in water at 287 nm with gradual increase in substrate (urea) concentration.

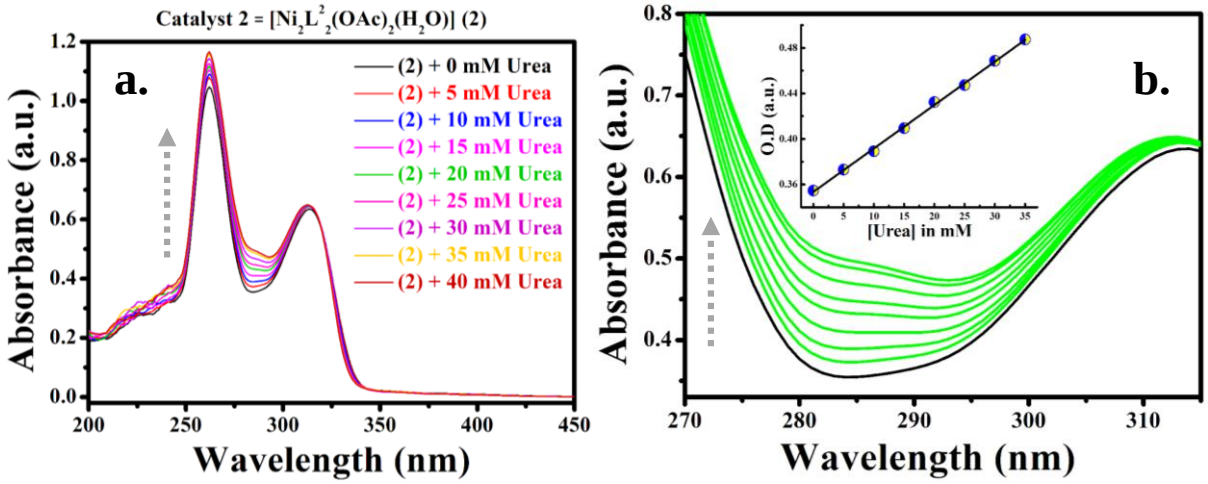

Figure S11. (a) Concentration dependent electronic spectral changes of the complex **2** (0.2 mM) in water under open atmosphere at 25 °C. The spectra were recorded at 40 s intervals. (b) Development of a new absorption band at 285 nm with continuous raise in optical density of **2** in water *via* gradual increase in substrate (urea) concentration. The inset shows the diagram of absorbance *vs* wavelength maximum at 285 nm.

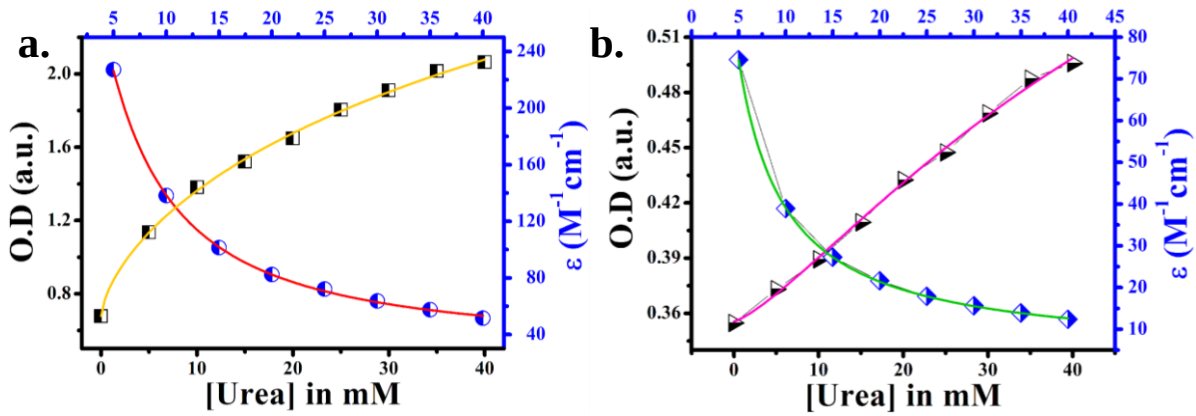

Figure S12. (a) Concentration dependent changes in absorbance (O.D) and molar extinction coefficient (wavelength maxima = 287 nm, ε in $M^{-1}cm^{-1}$) for complex **1** ([catalyst] = 0.2 mM and [urea] = 0 to 200 equiv.), (b) represents similar analysis as that of (a) for complex **2** (wavelength maxima = 285 nm).

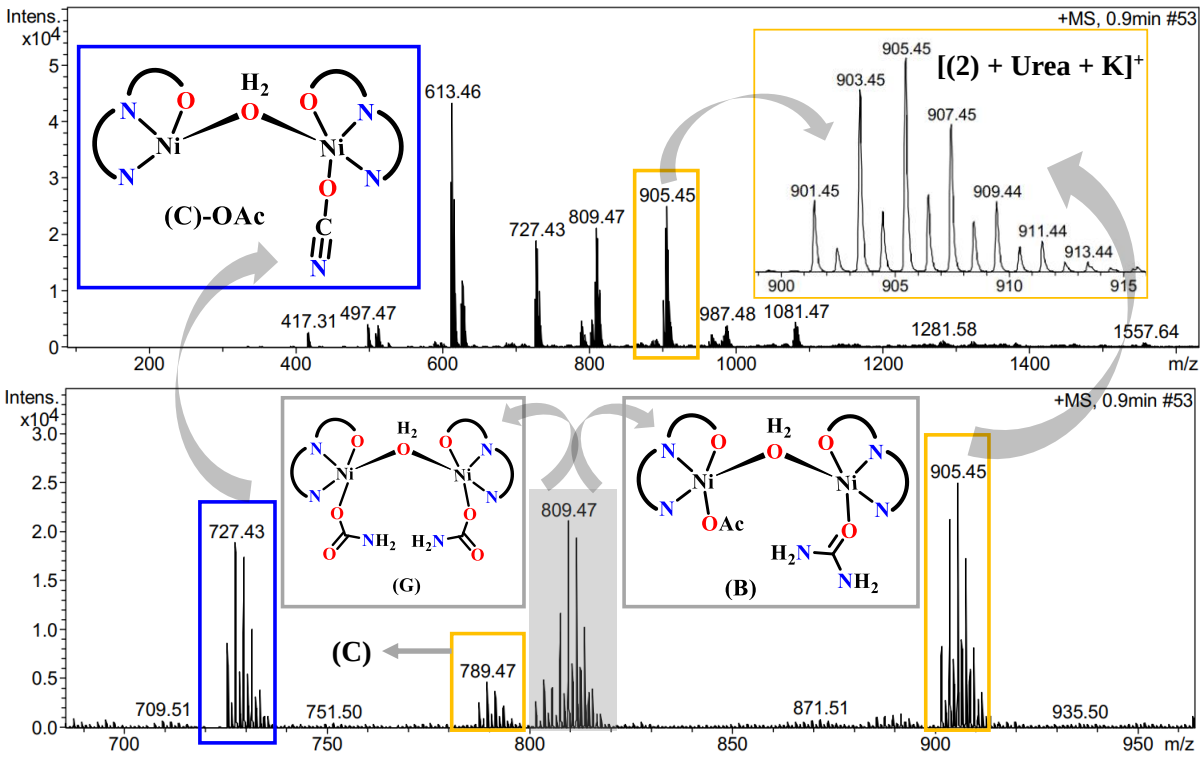

Figure S13. Identification of the intermediates during binding of urea to urease mimetic **2** through ESI-MS (in aqueous medium, m/z, +ve mode), catalyst **2**-2OAc+NCO = 727.43 i.e. intermediate **(B)** = 806.87, intermediate **(C)** = 788.83, intermediate **(C)**-OAc = 727.43, intermediate **(G)**+H^+ = 807.81 and {catalyst **2** +urea+K}$^+$ = 905.45, respectively. Intermediates are defined in Scheme S2. The ratio between catalyst **2** and urea is 1:100 and the data has been recorded after 1 h of mixing.

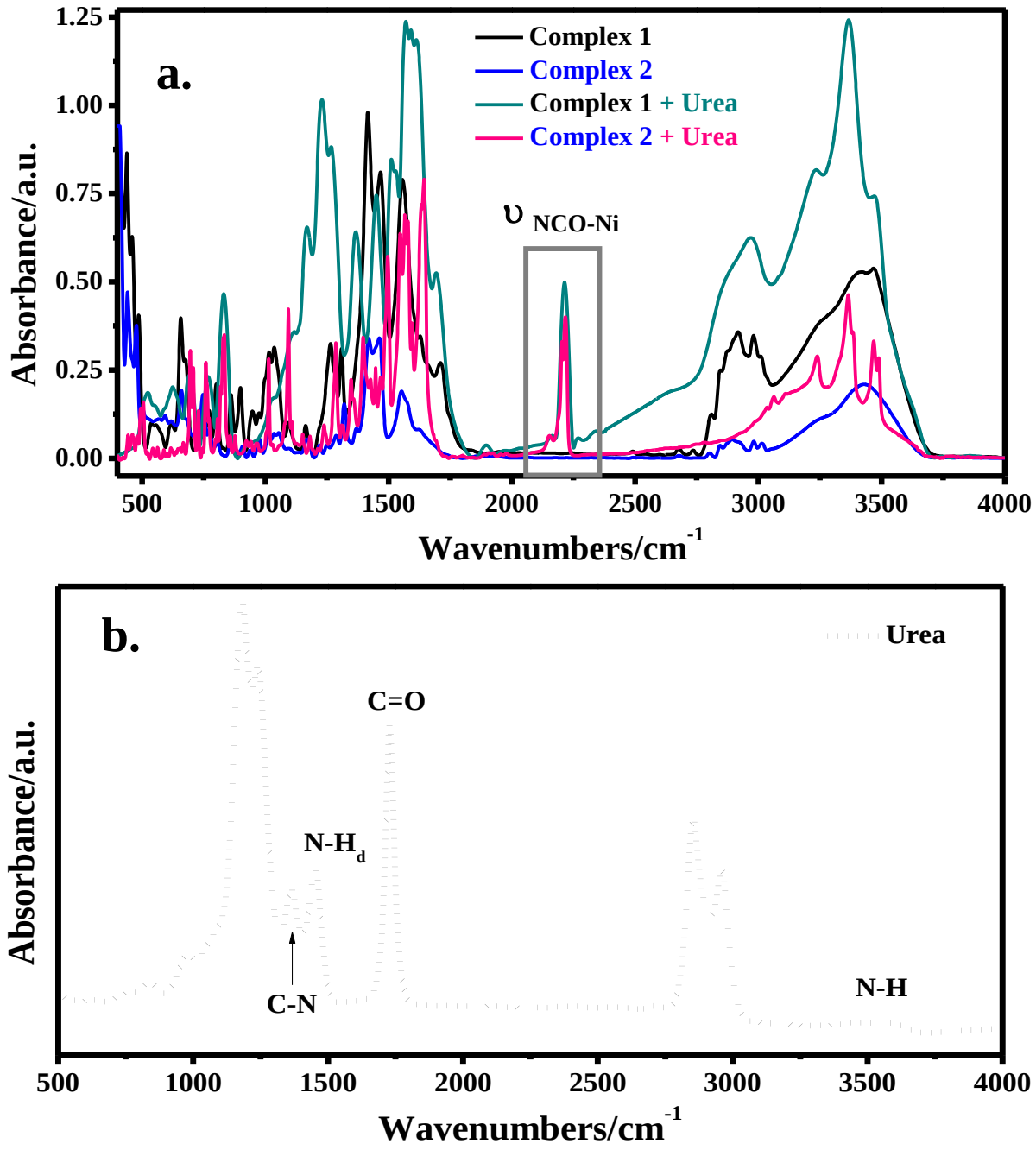

Figure S14. Infrared vibrational spectra of (a) the complexes and the reaction medium. Reaction was carried out between urea (2 mmol) and 0.02 mmol of each complex at 59 °C in aqueous medium for 2 h. Data were recorded using KBr pallets and represented as absorbance *vs* wavenumber (cm^{-1}). (b) FTIR spectrum of pure urea sample.

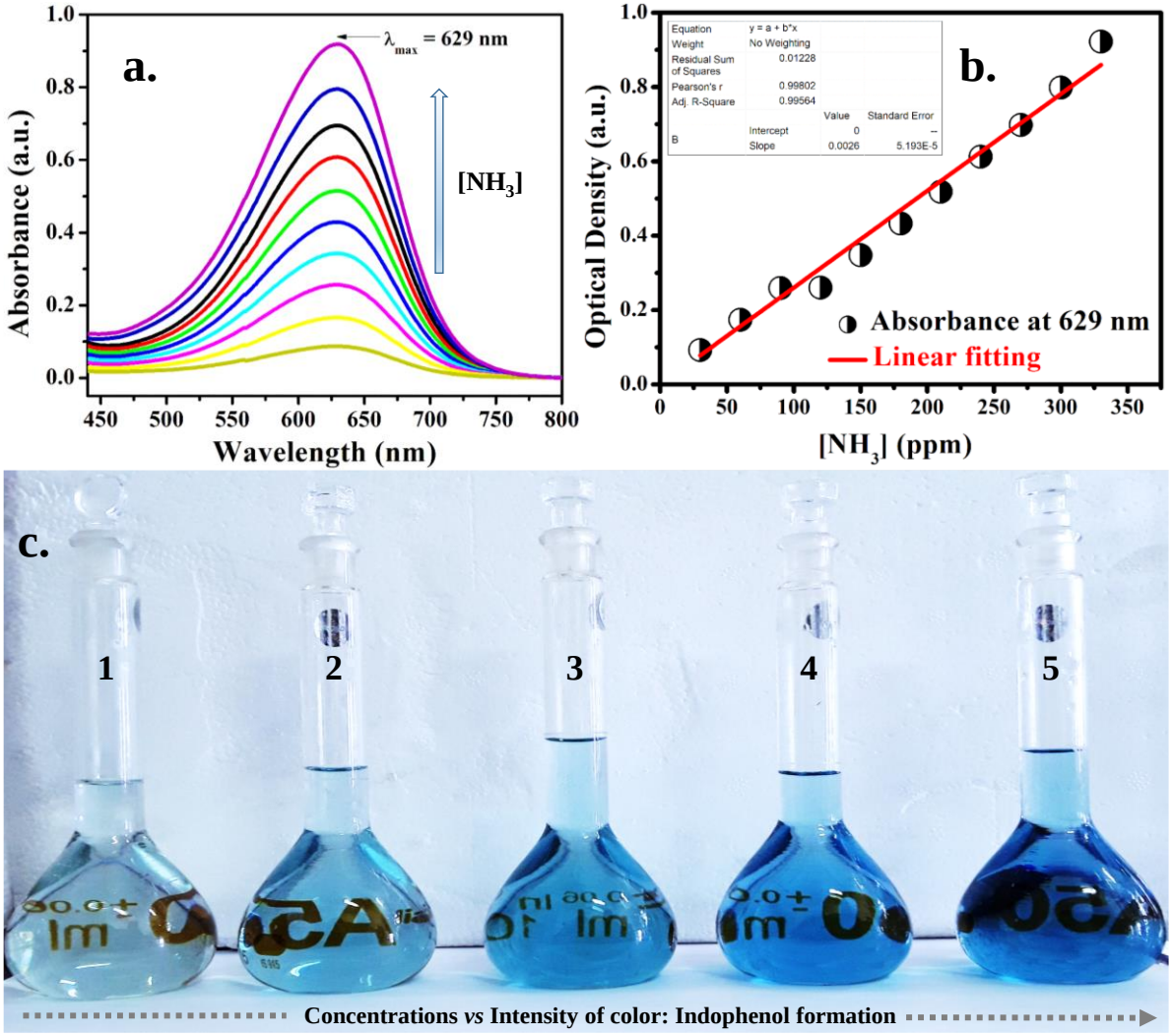

Figure S15. Modified indophenol method for colorimetric detection and quantification of ammonia (NH_3): (a) concentration dependent UV-Vis spectra of the indophenol at a characteristic wavelength maximum of 629 nm (formed *via* ammonia assay, Section S3.2, aliquots of standard ammonia solutions were in the range of 30-330 ppm). (b) Standard calibration curve fitted through straight line equation assuming intercept as 0. (c) The signature of the ammonia production by the gradual development of indophenol as described in the ammonia assay. **1-5** define the lower to higher concentrations of standard ammonia solutions (From left to right: 30, 90, 150, 210 and 300 ppm, respectively).

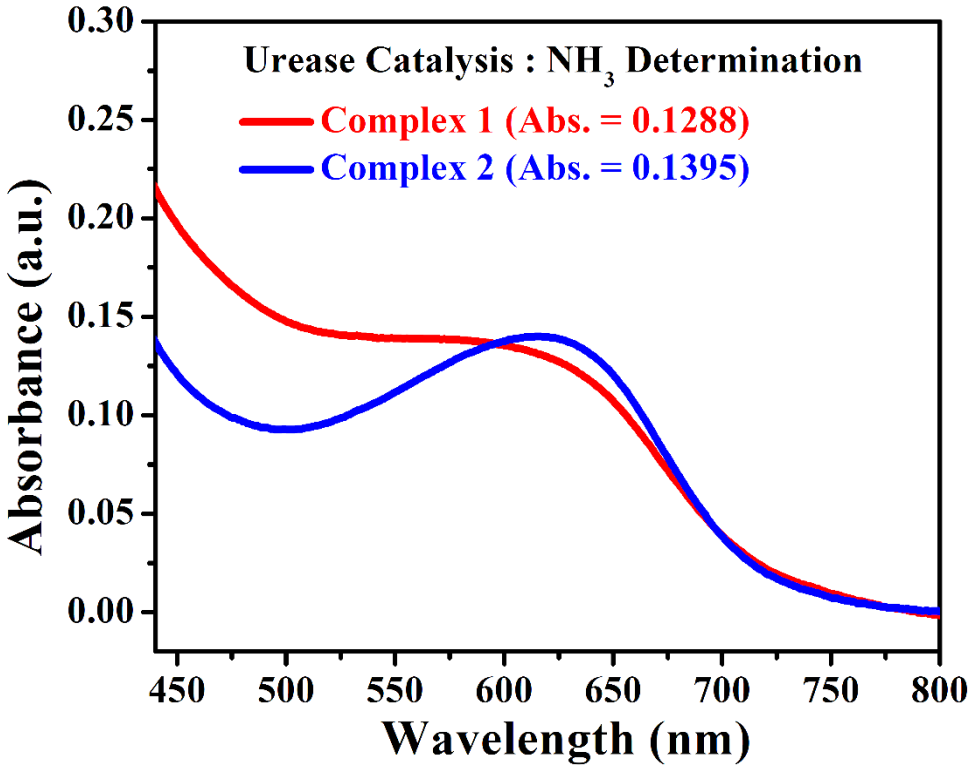

Figure S16. Ammonia (NH_3) measurement of unknown samples *via* modified indophenol method. Absorbance (Abs.) values considered at wavelength maximum of 629 nm for both complexes.

One-pot synthesis of AmCyPys

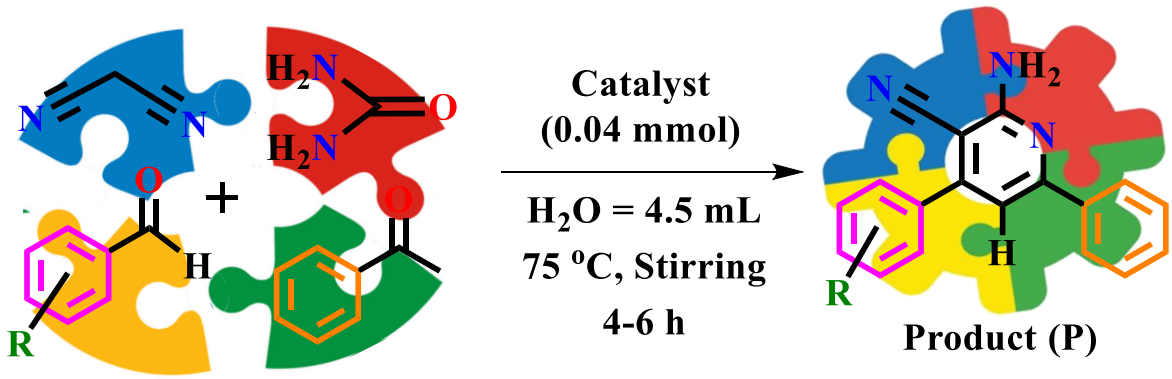

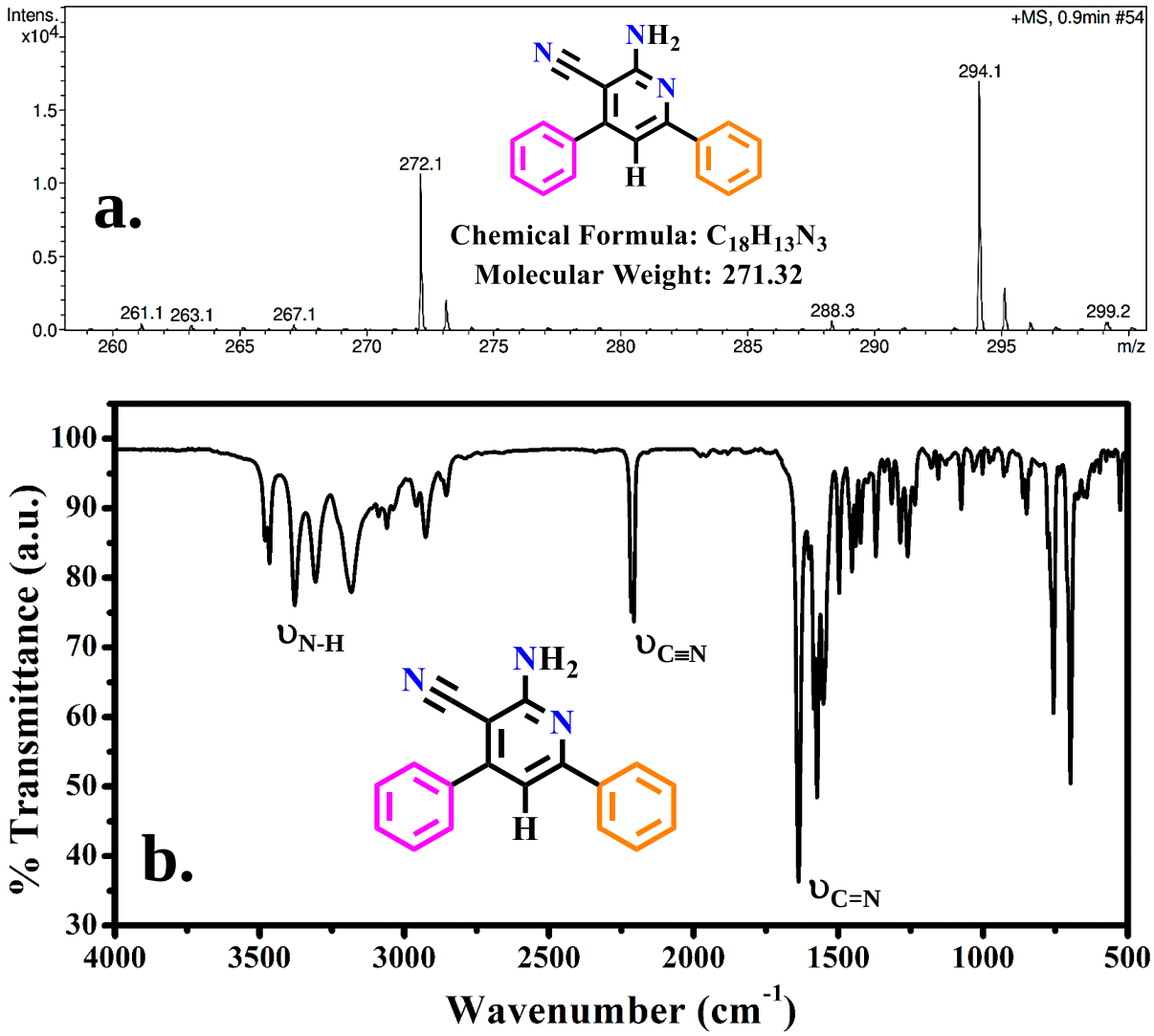

Figure S17. (a) ESI-MS spectra: molecular ion peak at M + H^+ = 272.1, M + Na^+ = 294.1 (in HPLC MeOH) and (b) FTIR spectra (KBr pallet) of **P-1**.

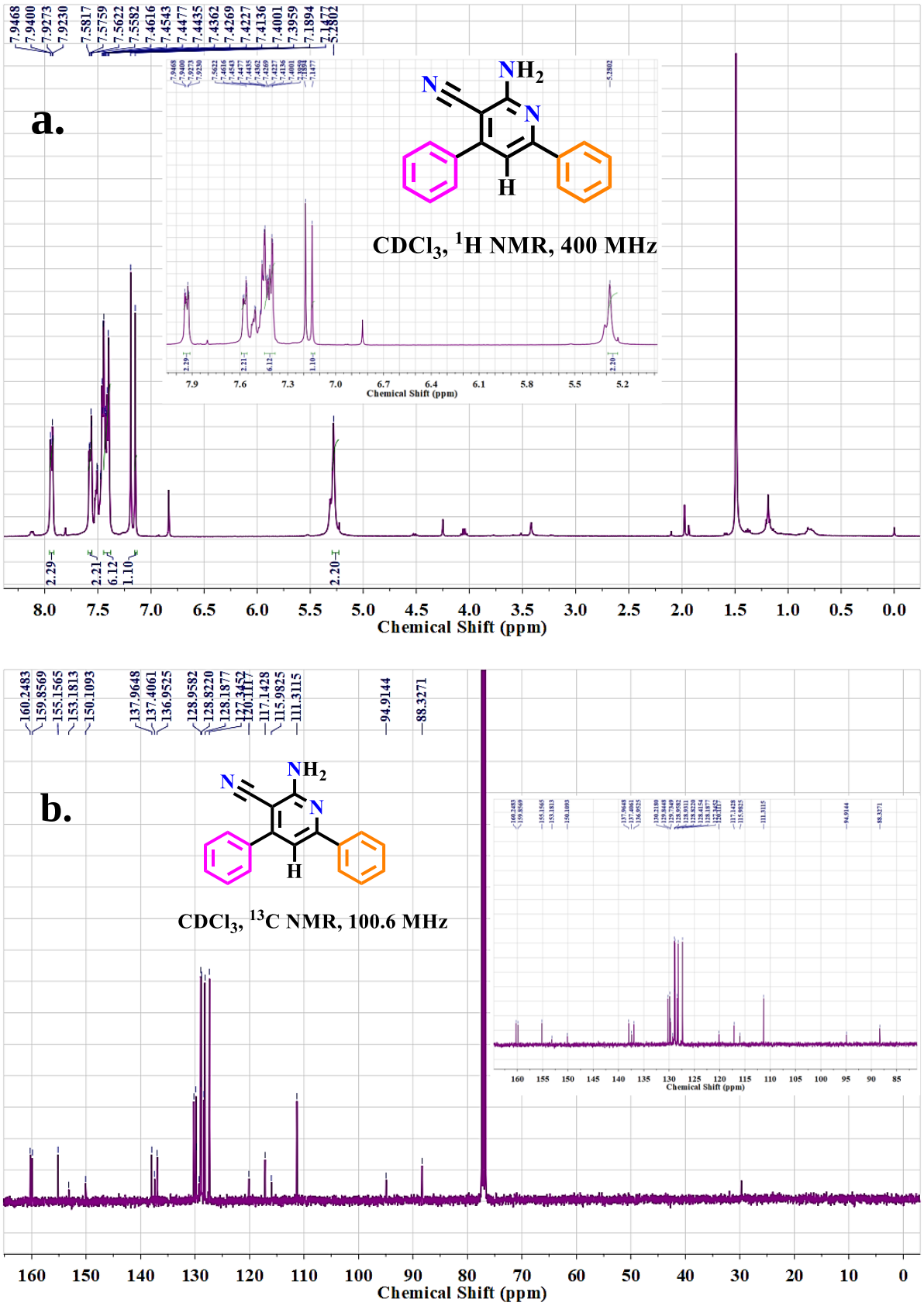

Figure S18. (a) ^{1}H NMR and (b) ^{13}C NMR of **P-1** (in chloroform-d, 25 °C).

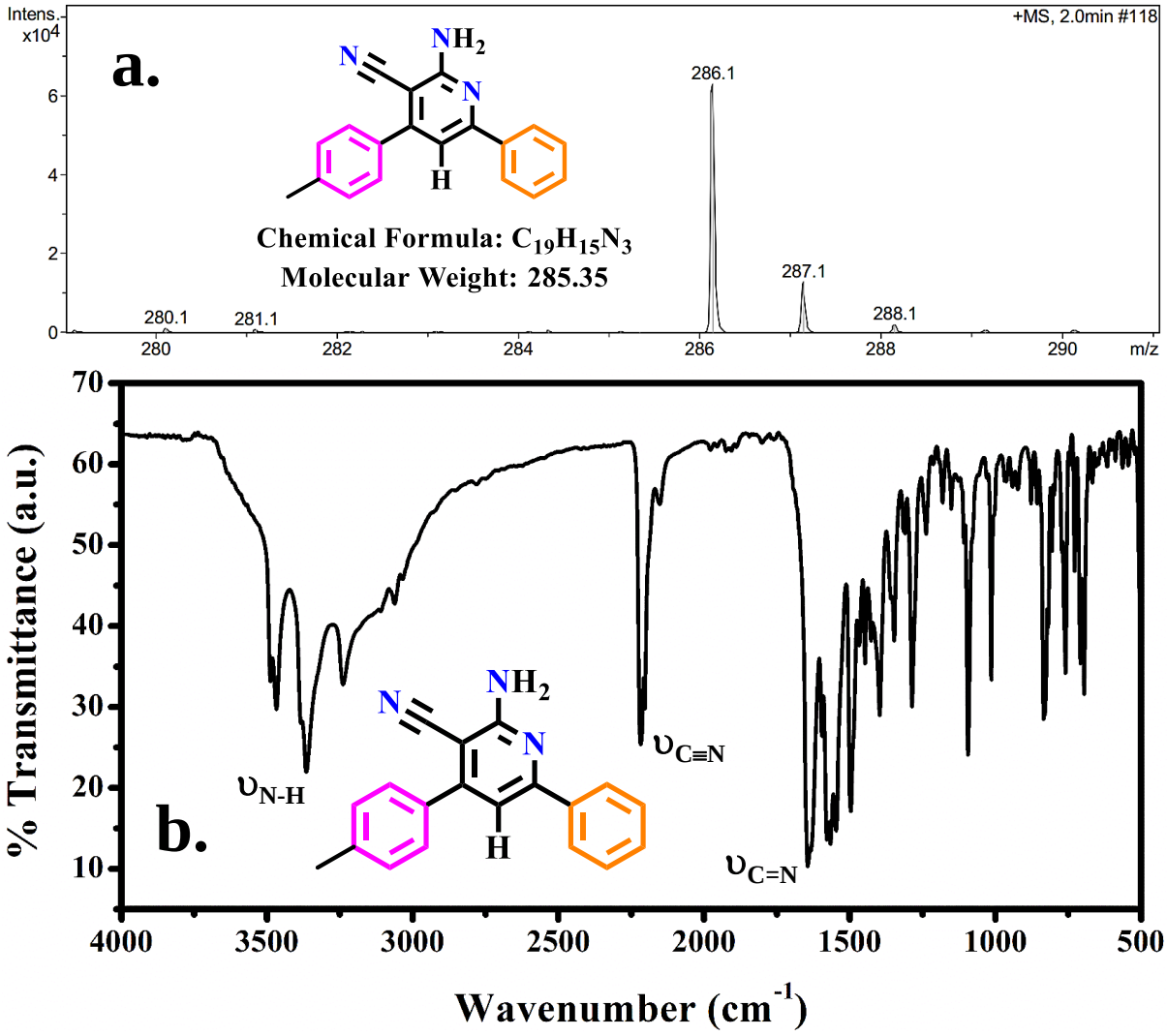

Figure S19. (a) ESI-MS spectra: molecular ion peak at M + H^+ = 286.1 (in HPLC MeOH) and (b) FTIR spectra (KBr pallet) of **P-2**.

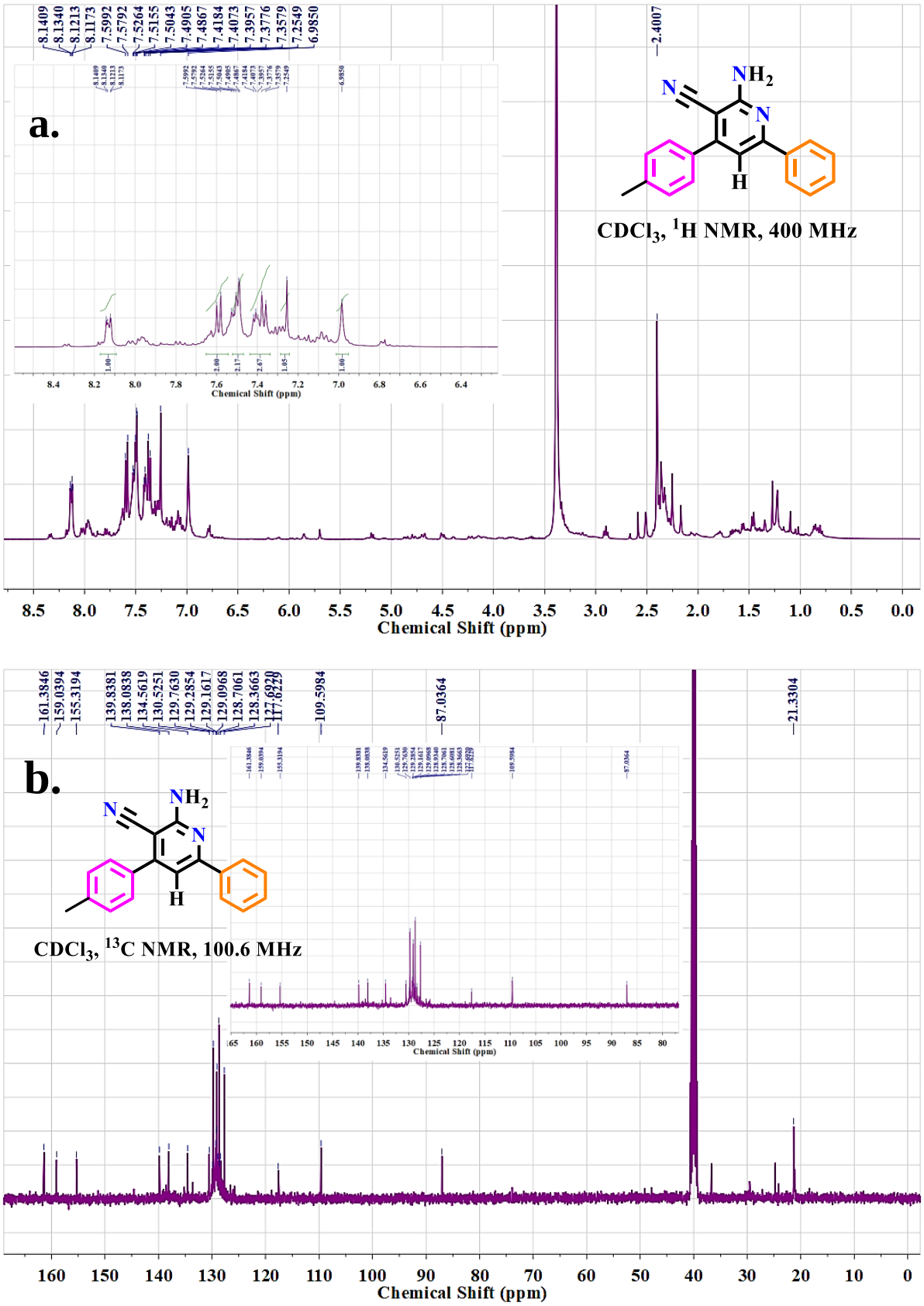

Figure S20. (a) ^{1}H NMR and (b) ^{13}C NMR of **P-2** (in chloroform-d, 25 °C).

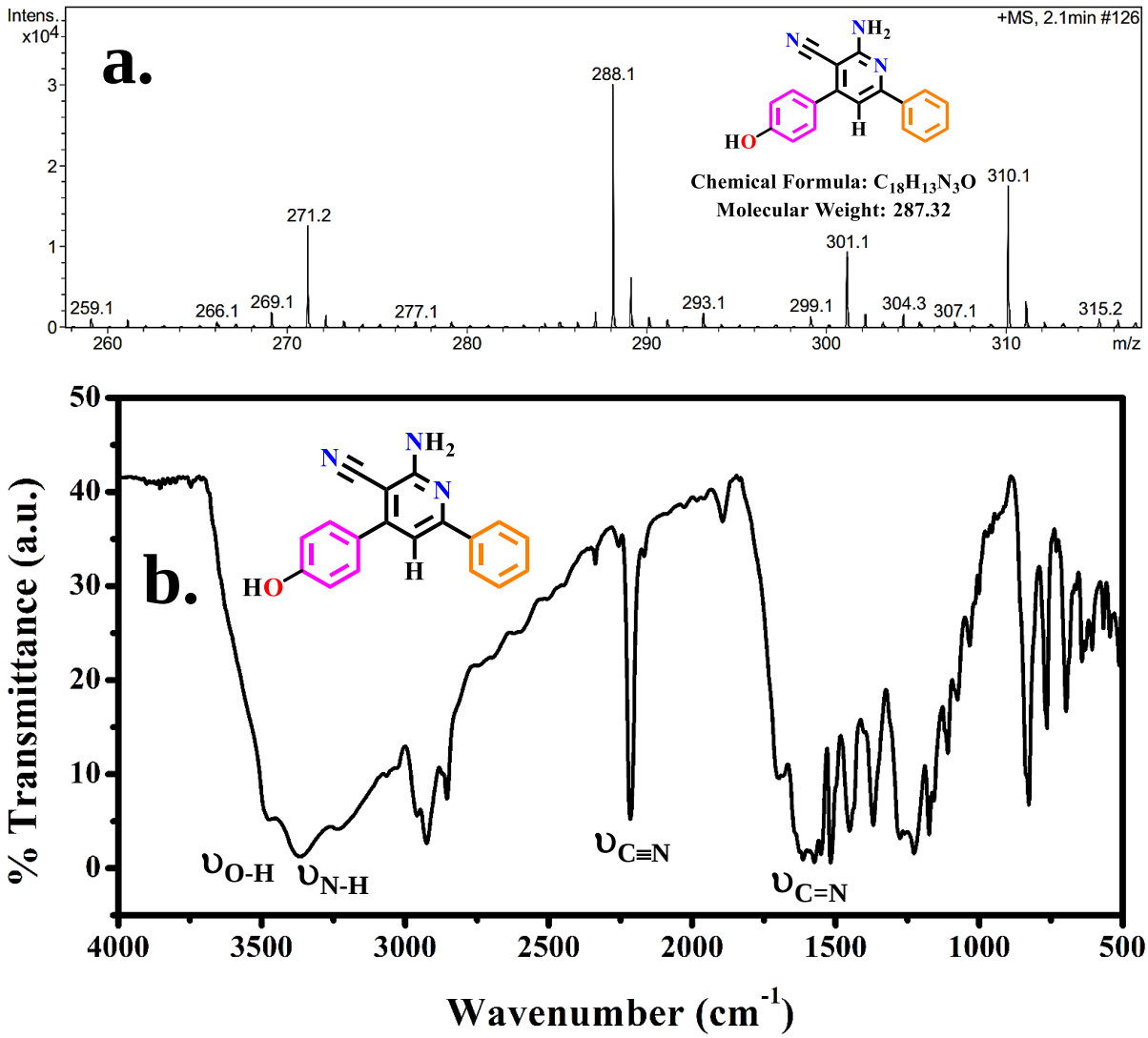

Figure S21. (a) ESI-MS spectra: molecular ion peak at M + H^+ = 288.1, M + Na^+ = 310.1 (in HPLC MeOH) and (b) FTIR spectra (KBr pallet) of **P-3**.

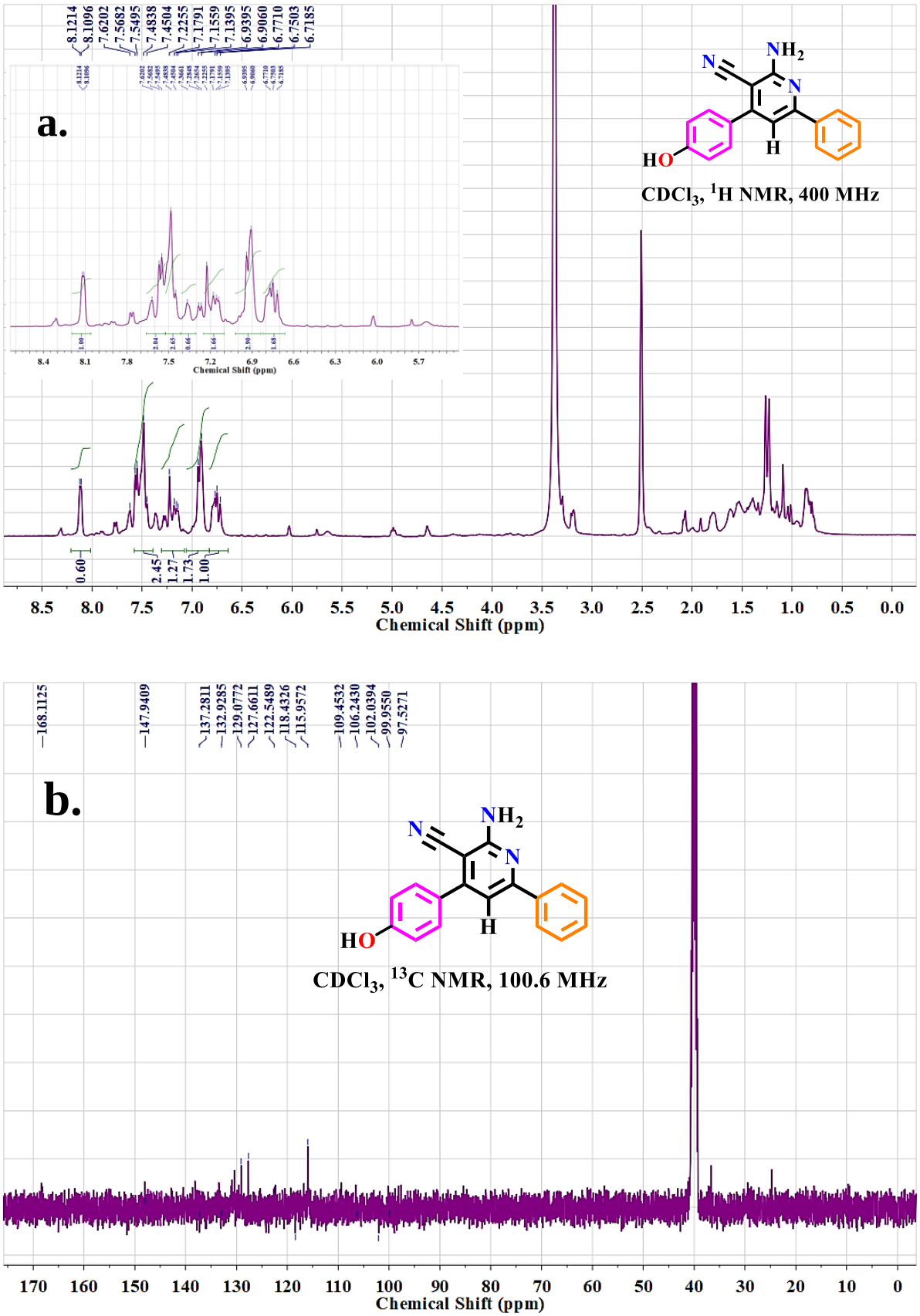

Figure S22. (a) ^{1}H NMR and (b) ^{13}C NMR of **P-3** (in chloroform-d, 25 °C).

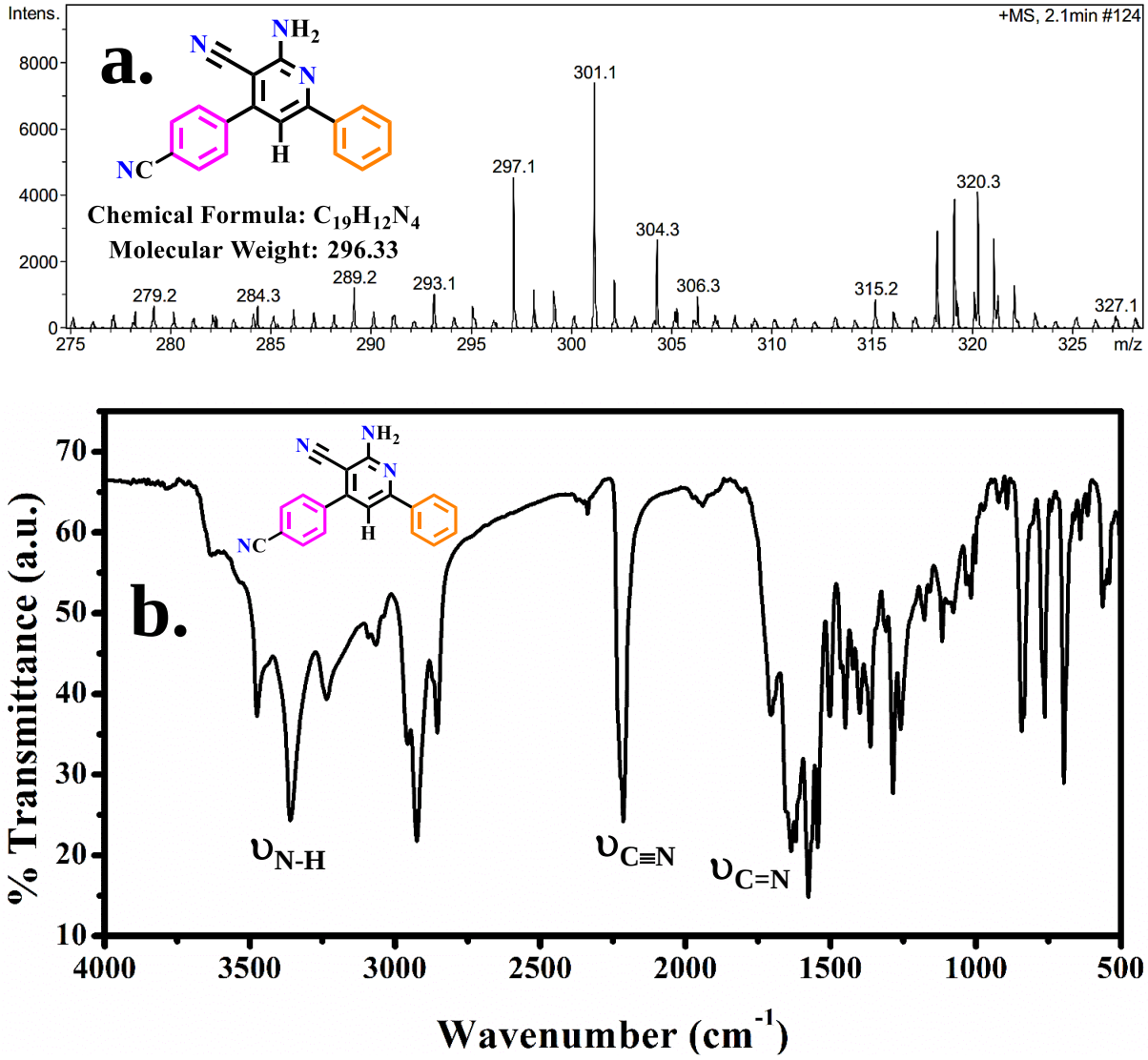

Figure S23. (a) ESI-MS spectra: molecular ion peak at M + H^+ = 297.1, M + Na^+ = 319.3 (in HPLC MeOH) and (b) FTIR spectra (KBr pallet) of **P-4**.

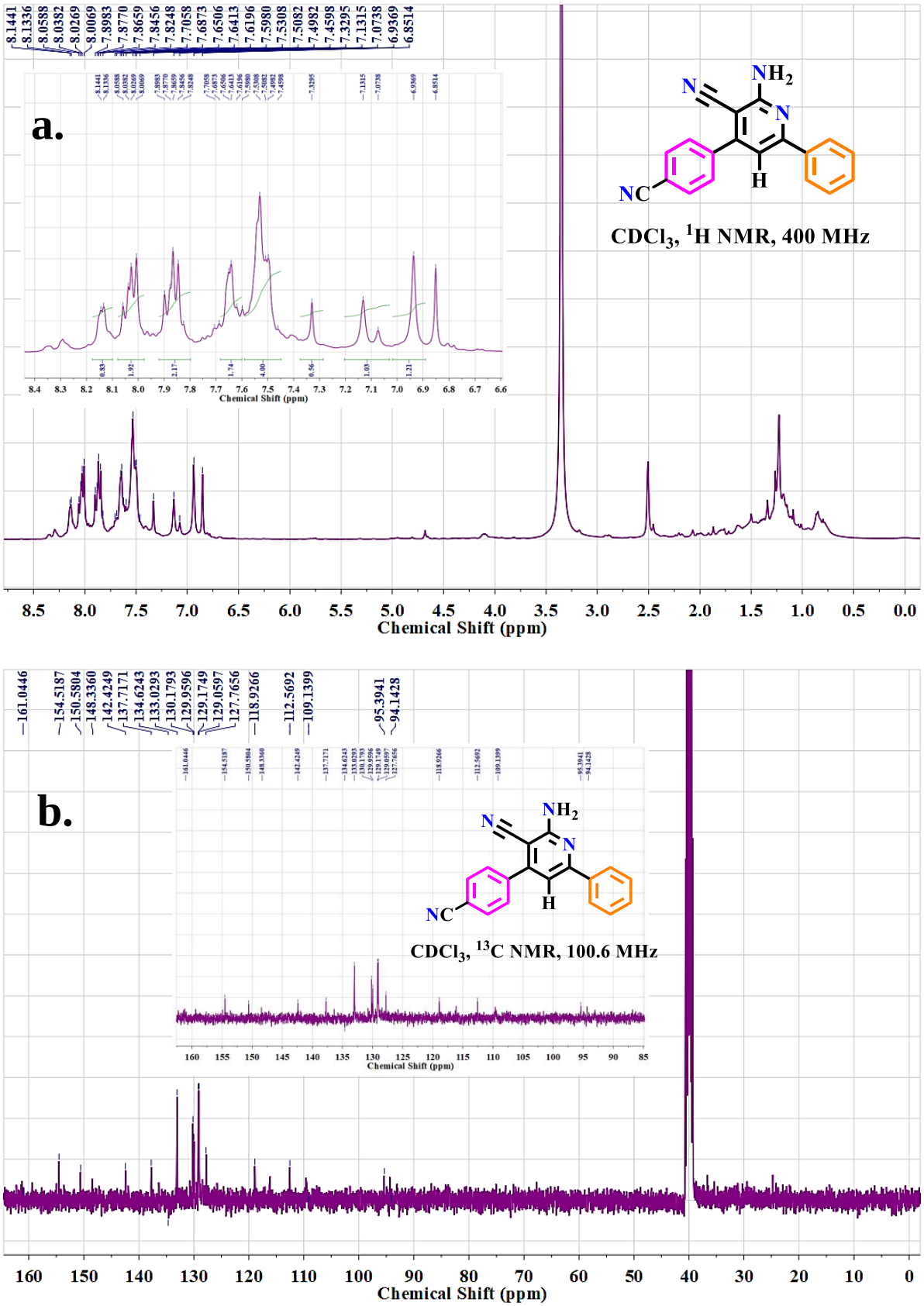

Figure S24. (a) ^{1}H NMR and (b) ^{13}C NMR of **P-4** (in chloroform-d, 25 °C).

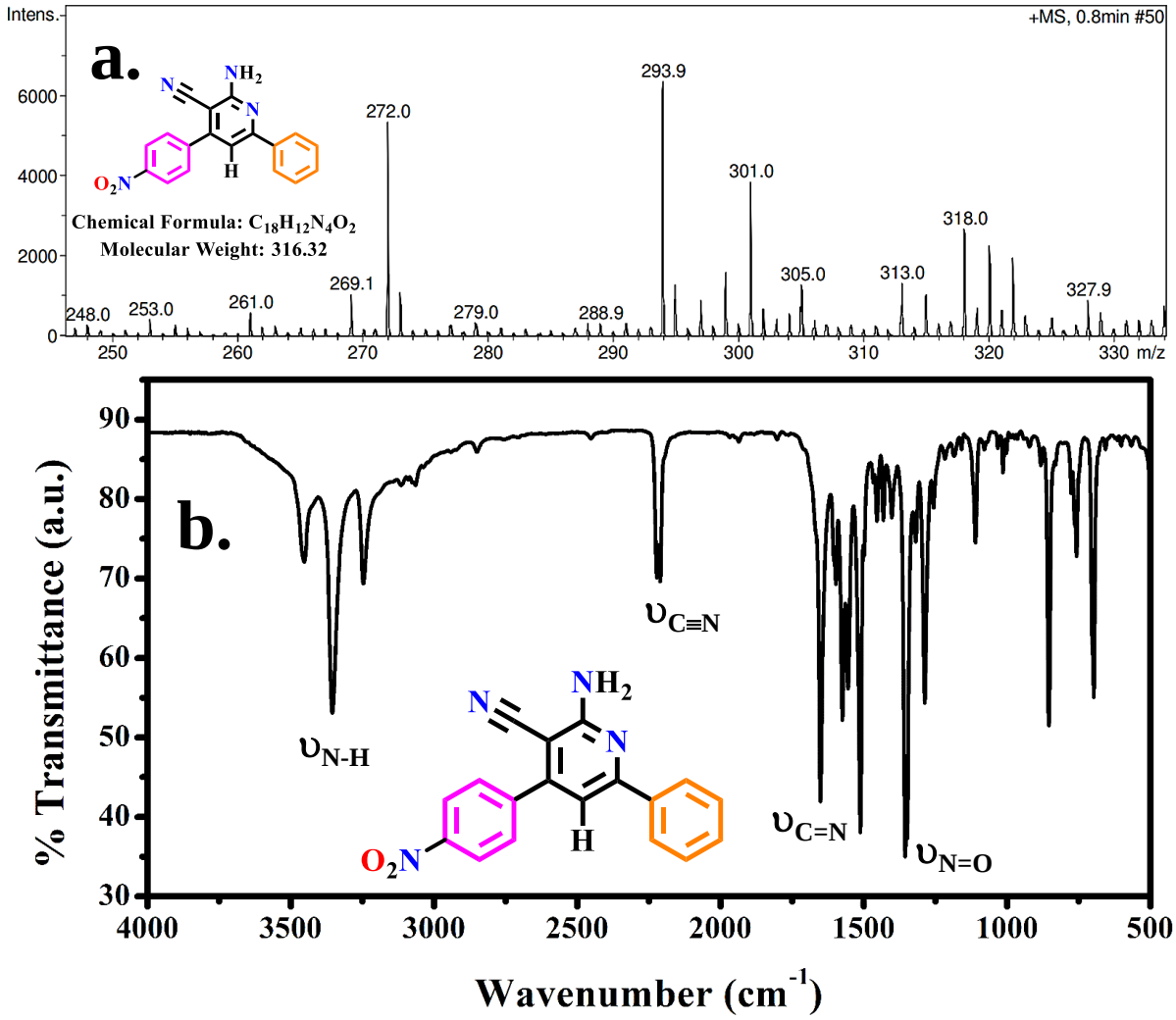

Figure S25. (a) ESI-MS spectra: molecular ion peak at M + H^+ = 318.0 (in HPLC MeOH) and (b) FTIR spectra (KBr pallet) of **P-5**.

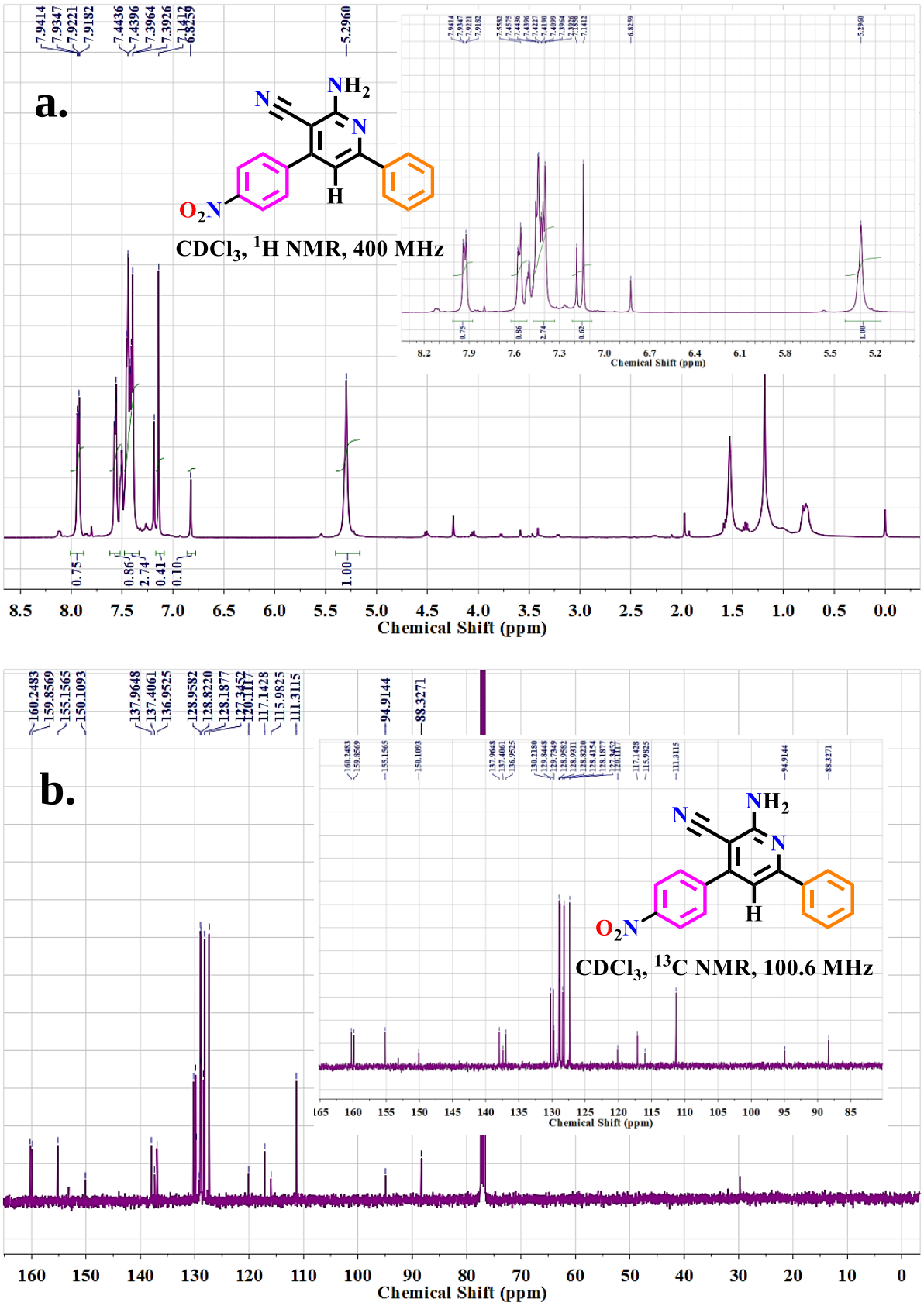

Figure S26. (a) ^{1}H NMR and (b) ^{13}C NMR of **P-5** (in chloroform-d, 25 °C).

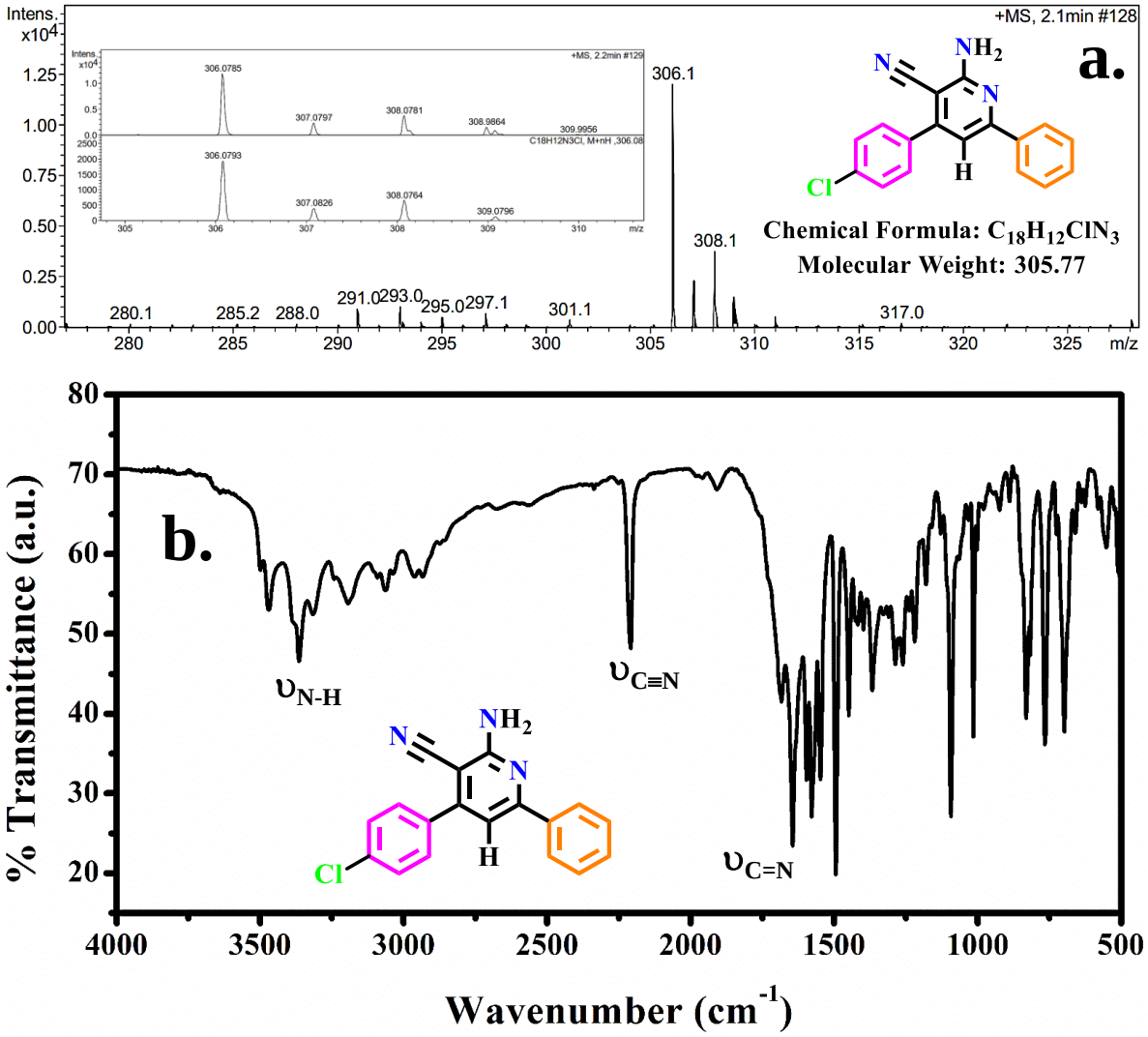

Figure S27. (a) ESI-MS spectra: molecular ion peak at M + H^+ = 306.1 and (M+2) + H^+ = 308.1 responsible for -Cl pattern (in HPLC MeOH) and (b) FTIR spectra (KBr pallet) of **P-6**.

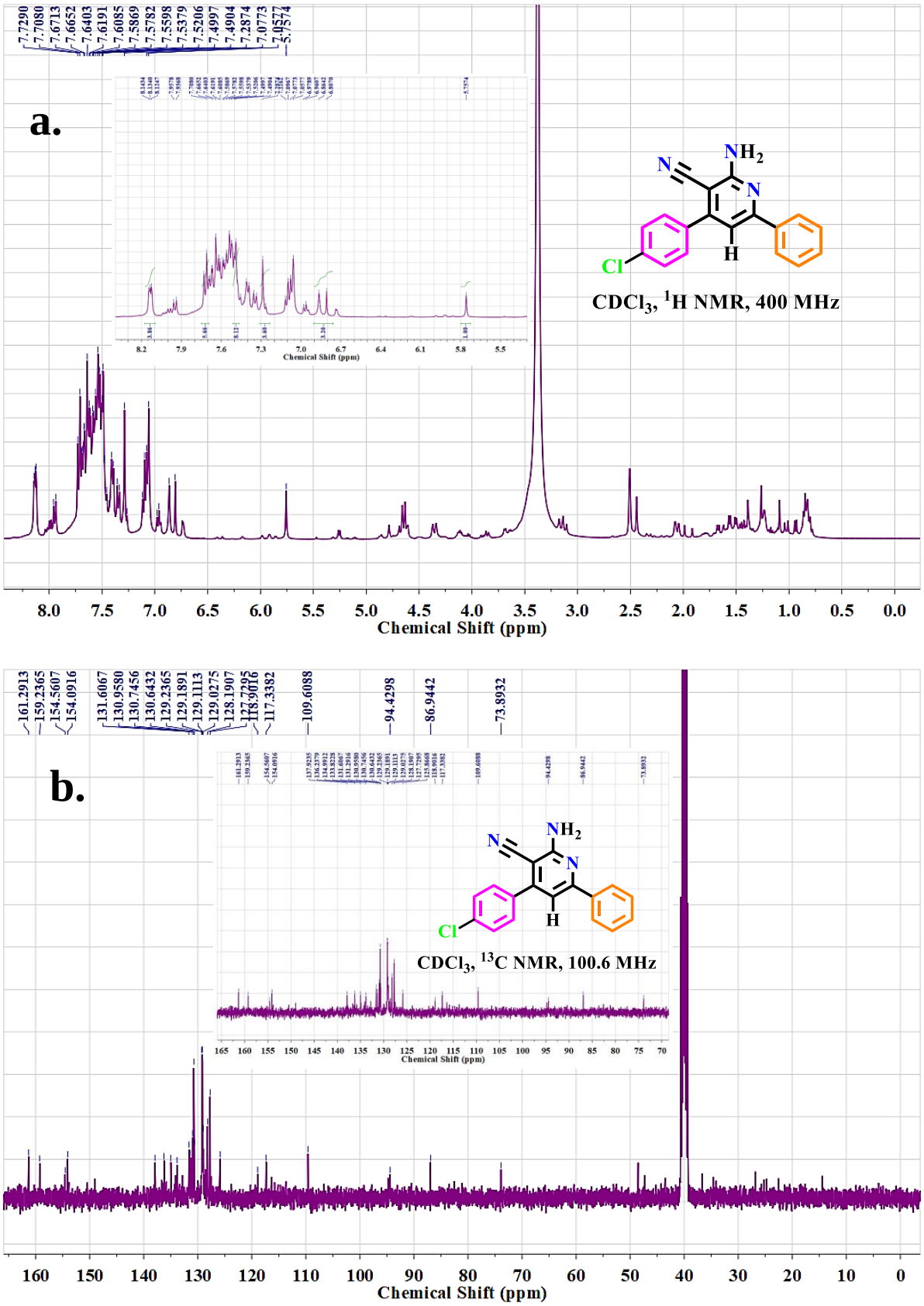

Figure S28. (a) ^{1}H NMR and (b) ^{13}C NMR of **P-6** (in chloroform-d, 25 °C).

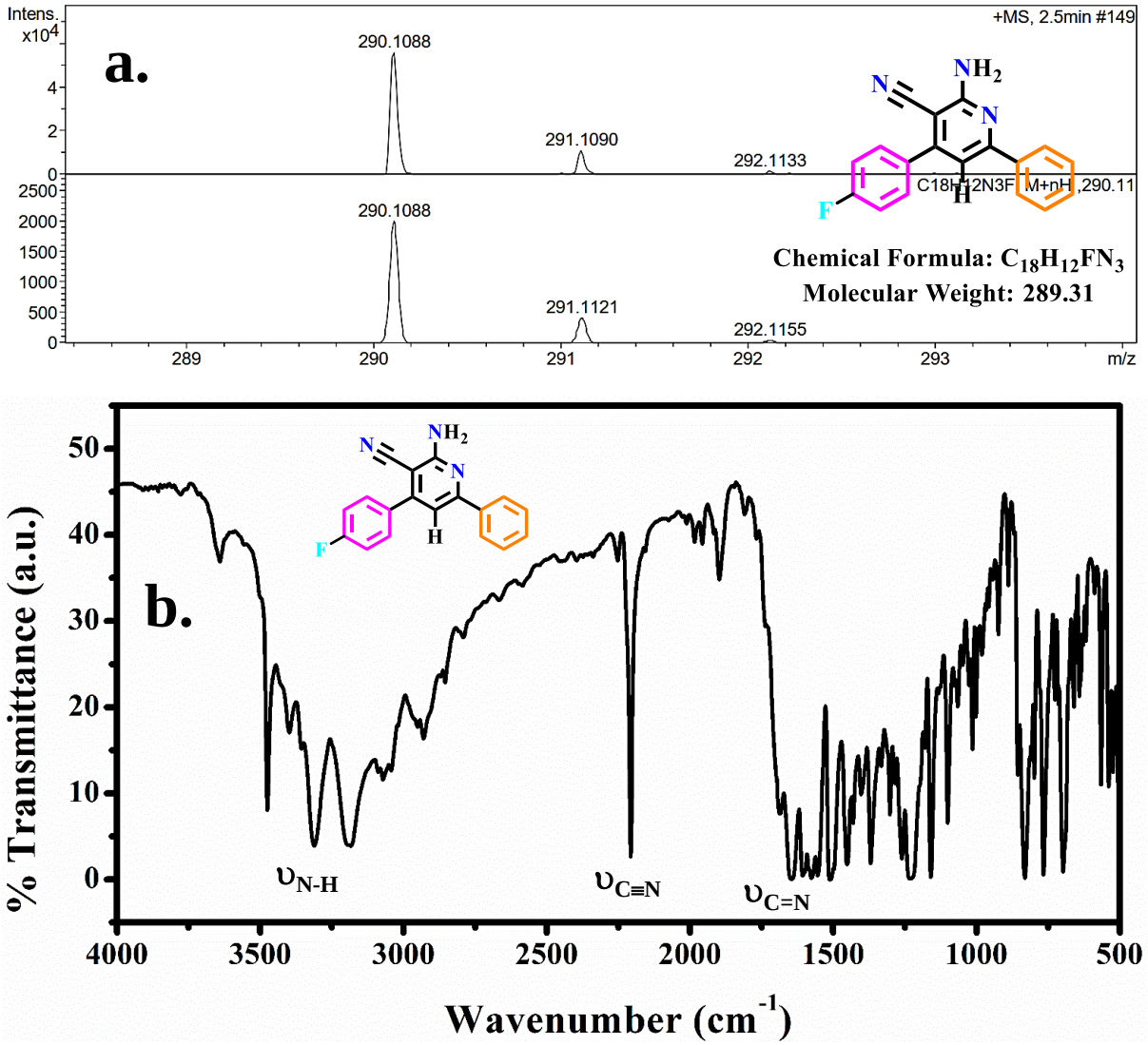

Figure S29. (a) ESI-MS spectra: molecular ion peak at M + H^+ = 290.1 (in HPLC MeOH) and (b) FTIR spectra (KBr pallet) of **P-7**.

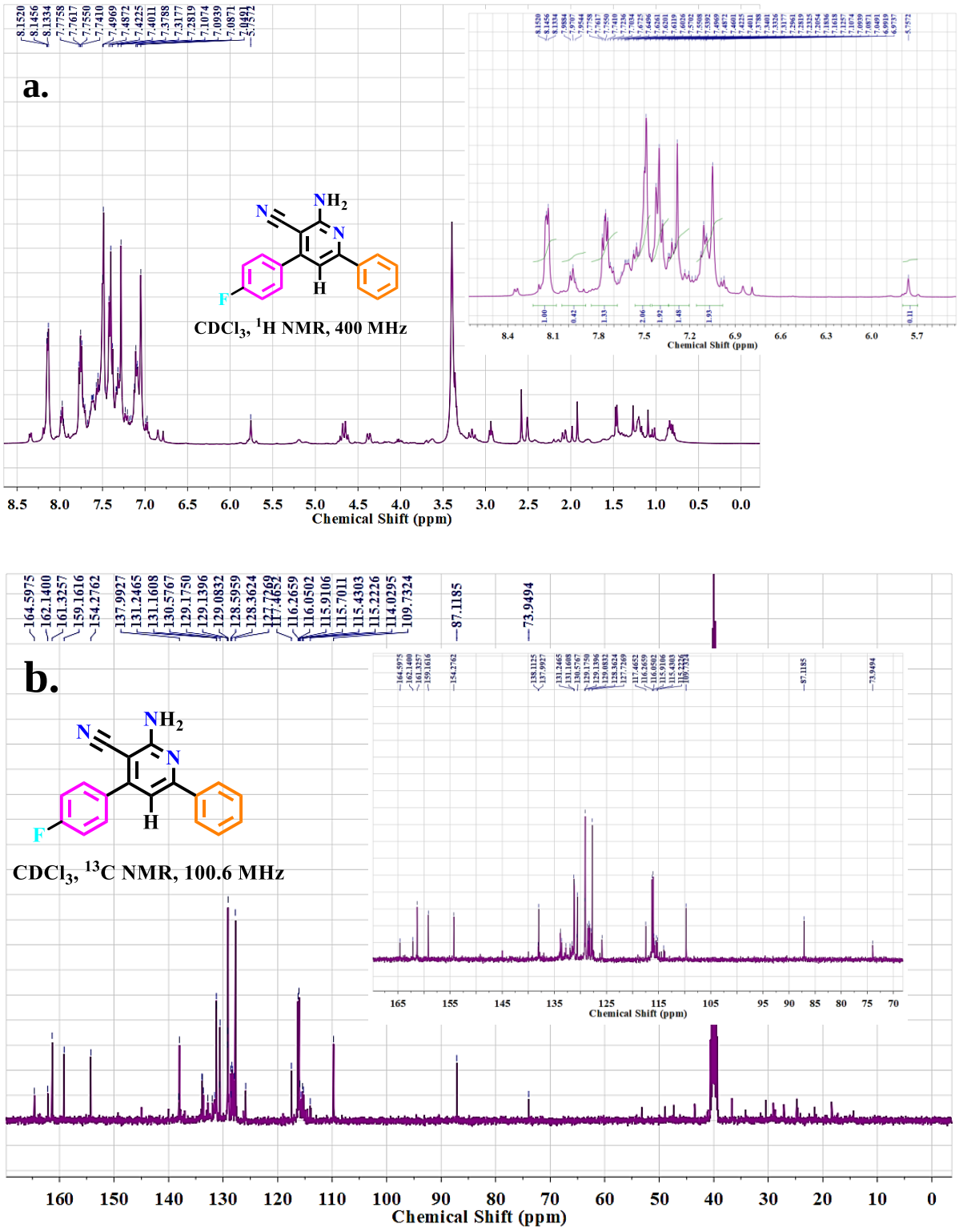

Figure S30. (a) ^{1}H NMR and (b) ^{13}C NMR of **P-7** (in chloroform-d, 25 °C).

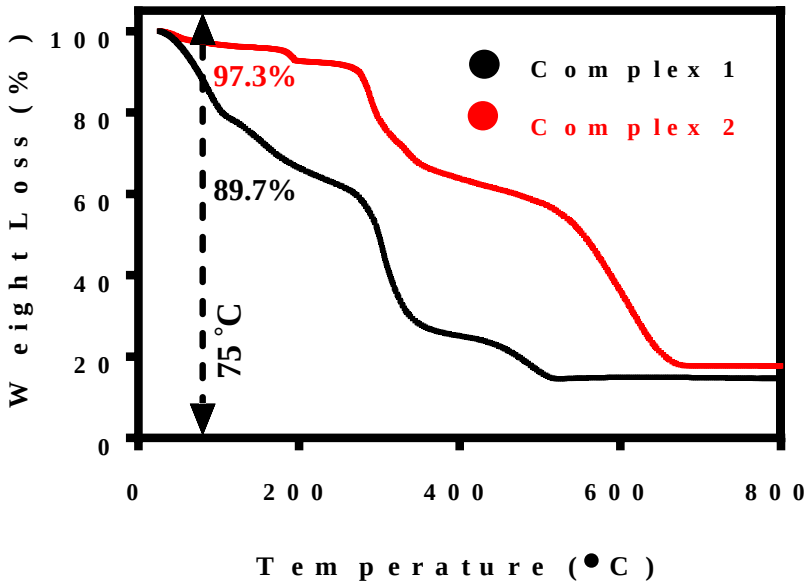

Figure S31. Thermal stability diagram of synthesized urease mimetics by TGA analysis. At catalytic temperature (T = 75 °C), complex **1** decomposes more rapidly with respect to its analogous **2**.

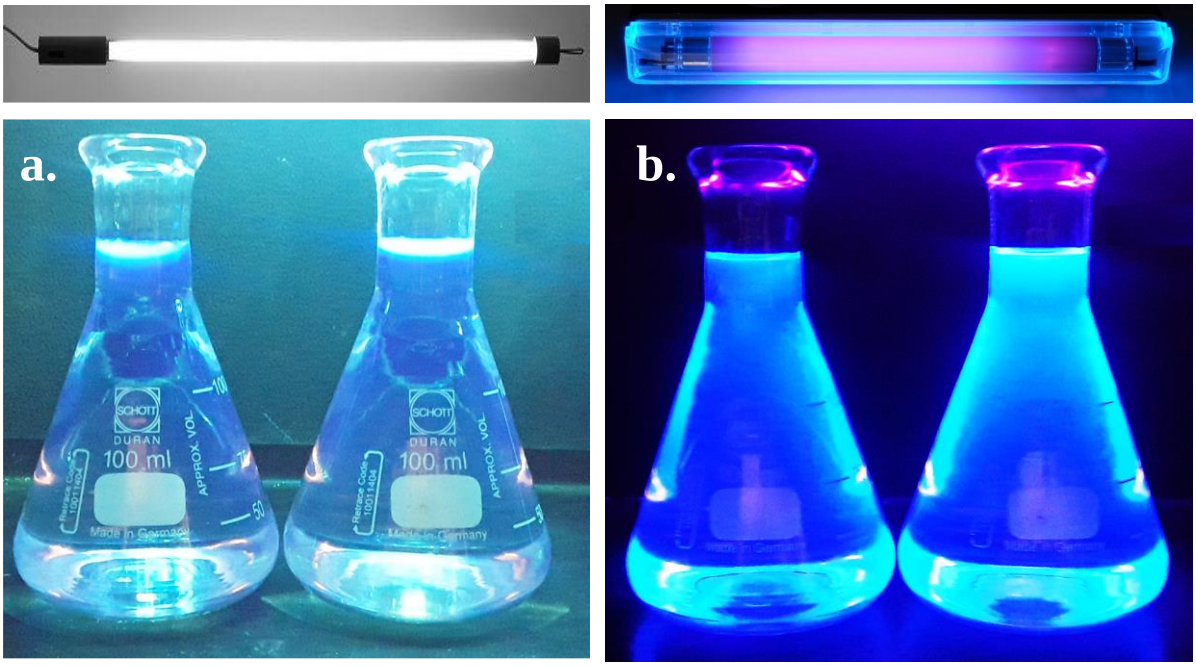

Figure S32. Normal (left) and UV (right) light incorporated hand-held camera images of **P-1** solution in aqueous phase.

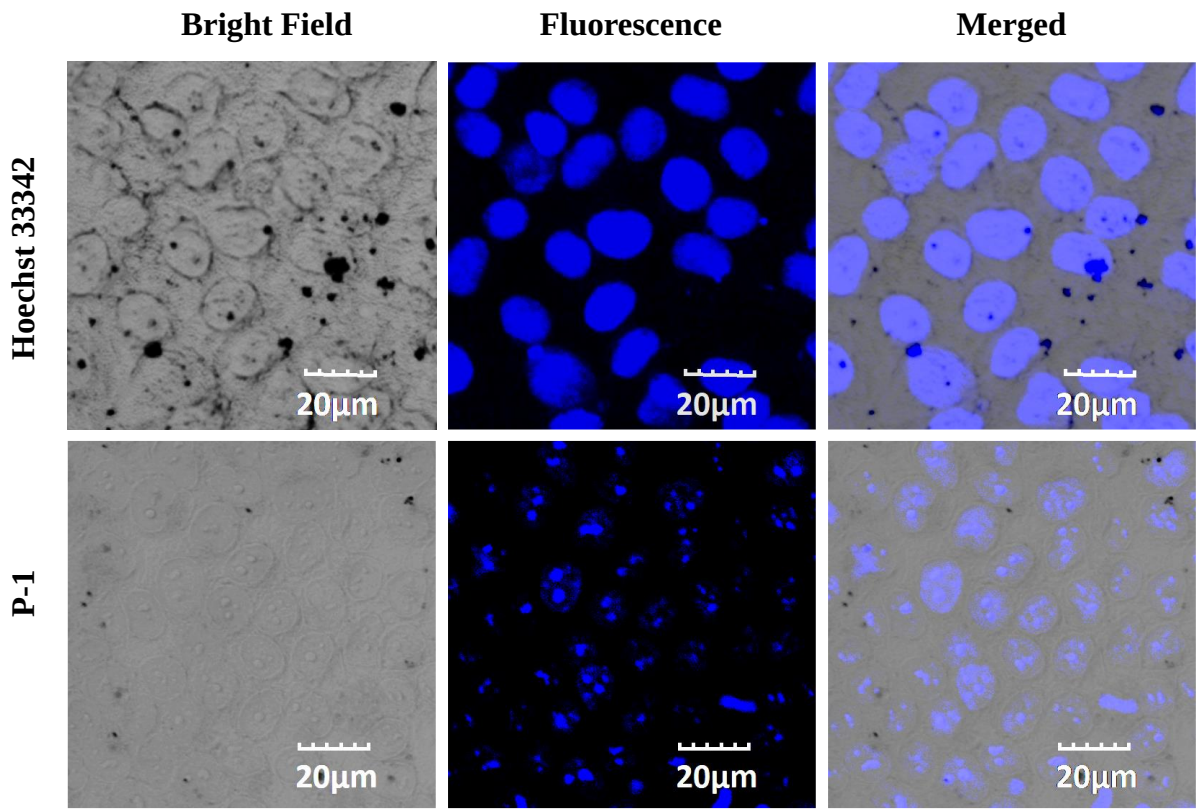

Figure S33. Confocal laser scanning microscopy (CLSM) images of human cervical cancer cell (HeLa) lines. This shows the site selection ability of the synthesized AmCyPYs (here P-1) in contrast to the reported cancer cell staining dye *viz.* Hoechst 33342.

Section S5. Schemes

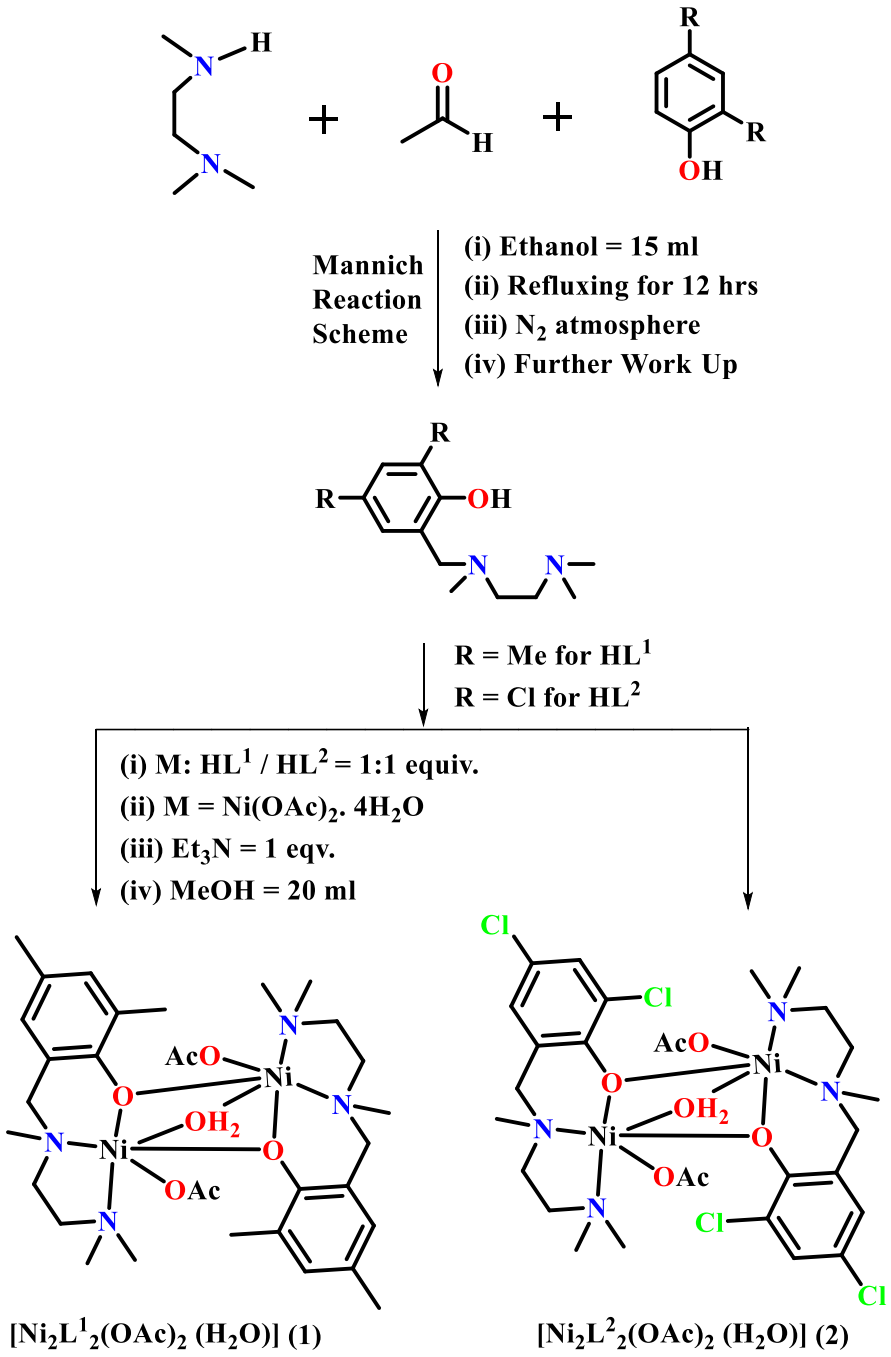

Scheme S1. Syntheses of Mannich base ligands, **HL**$^{1/2}$ and corresponding urease mimetics.

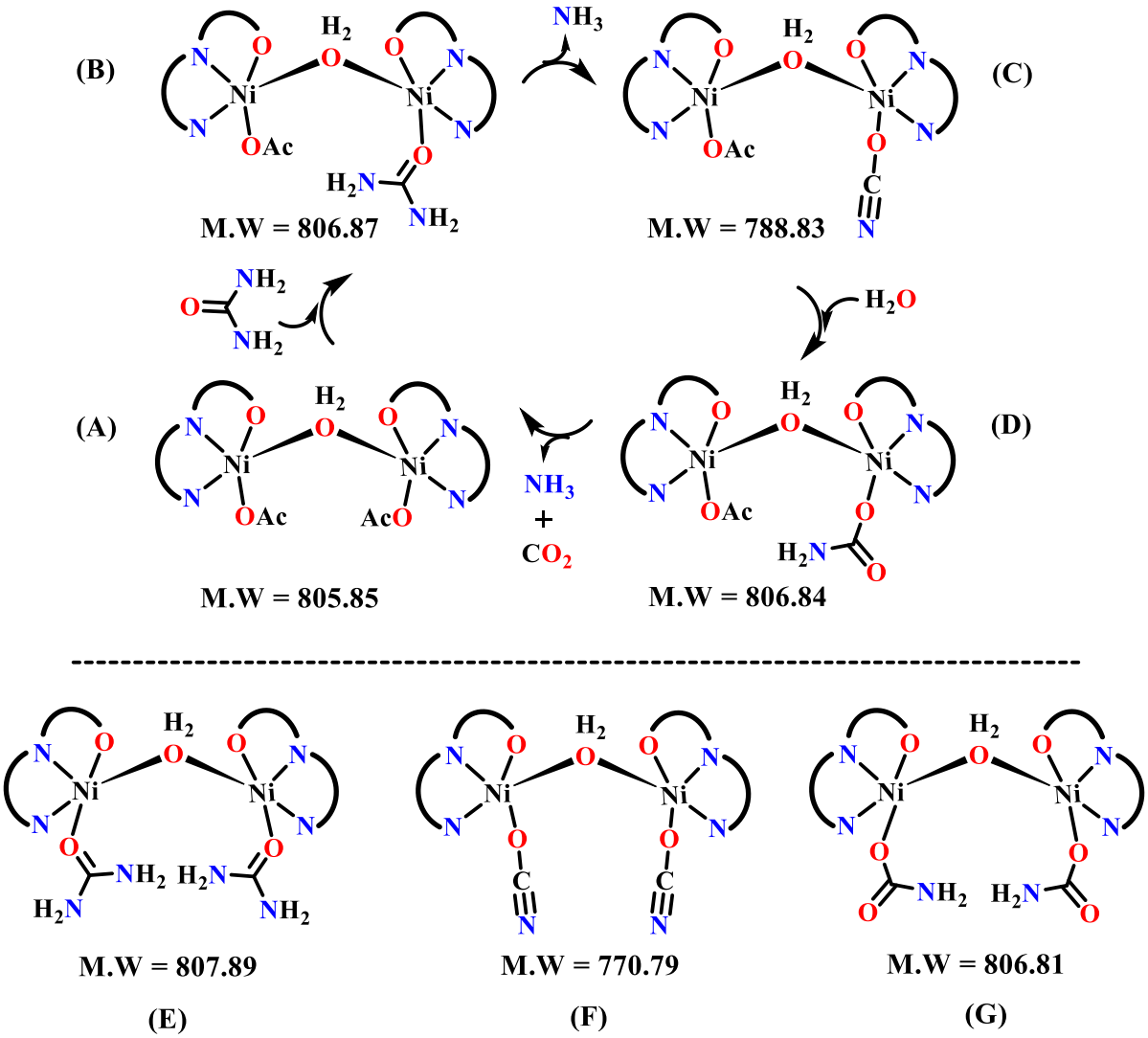

Scheme S2. Interactions between urea and dinickel centres in case of mimetic **2**.

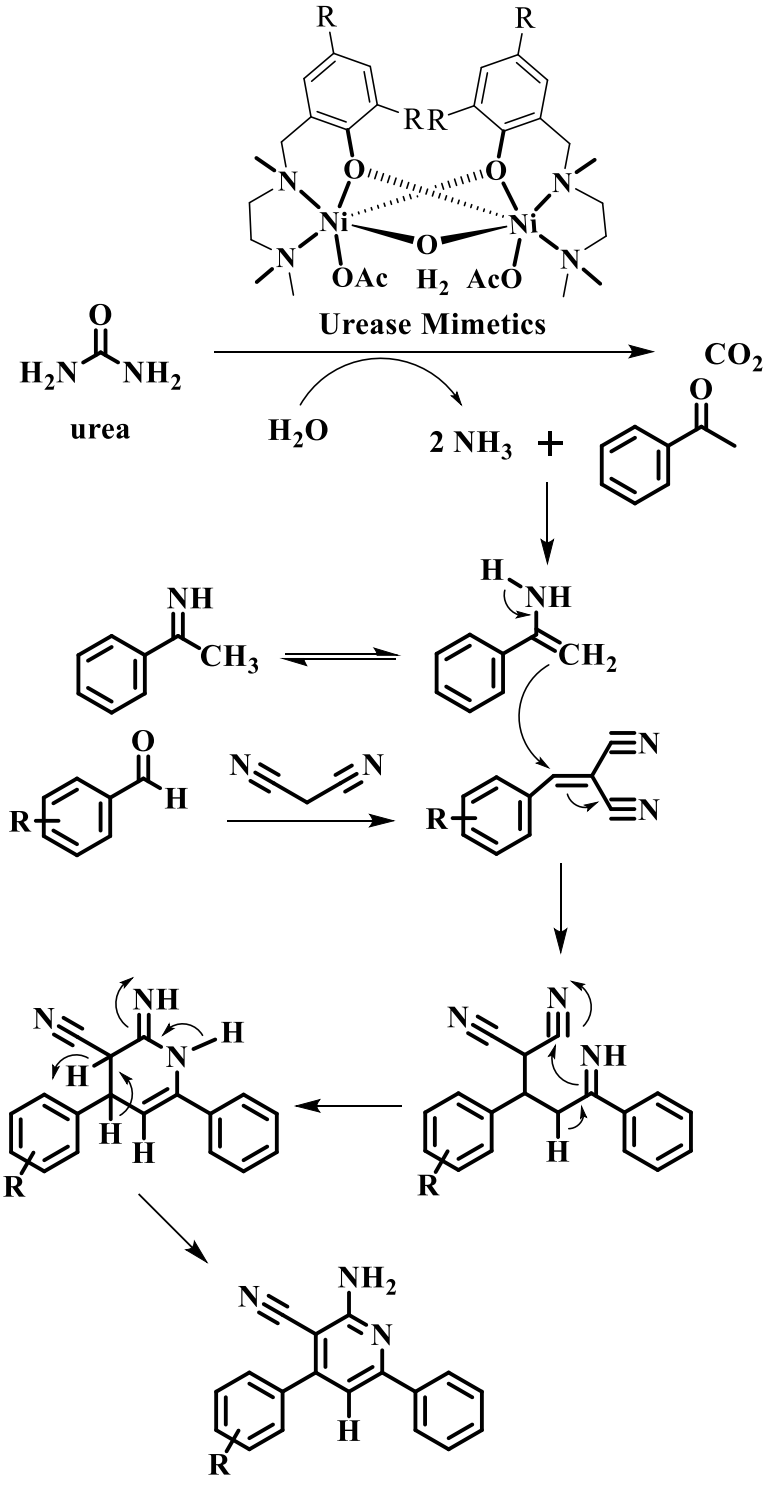

Scheme S3. Plausible mechanism for urease mimetics catalyzed synthesis of 2-amino-3-cyanopyridines (AmCyPys).

Section S6. Tables

Table S1. Selected bond lengths (Å) and bond angles (°) for complexes **1** and **2**.

$Ni_2L^1{}_2(OAc)_2(H_2O)$ (1)		*$Ni_2L^2{}_2(OAc)_2(H_2O)$ (2)*	
Ni(1)-Ni(1)#1	2.8222(6)	**Ni(1)-Ni(2)**	2.8773(10)
Ni(1)-O(1)	2.0359(17)	**Ni(1)-O(2)**	2.020(4)
Ni(1)-O(2)	2.0428(18)	**Ni(1)-O(1)**	2.052(4)
Ni(1)-N(1)	2.091(2)	**Ni(1)-O(7)**	2.072(4)
Ni(1)-O(4)	2.0927(19)	**Ni(1)-N(1)**	2.083(5)
Ni(1)-N(2)	2.150(3)	**Ni(1)-N(2)**	2.139(6)
Ni(1)-O(1)#1	2.1775(19)	**Ni(1)-O(4)**	2.292(4)
O(1)-Ni(1)#1	2.181(2)	**Ni(2)-O(5)**	2.015(5)
O(4)-Ni(1)#1	2.090(2)	**Ni(2)-O(4)**	2.029(4)
O(1)-C(1)	1.338(3)	**Ni(2)-O(7)**	2.060(4)
O(2)-C(10)	1.260(4)	**Ni(2)-N(3)**	2.079(5)
O(3)-C(10)	1.253(4)	**Ni(2)-N(4)**	2.152(6)
O(1)-Ni(1)-O(2)	170.98(8)	**Ni(2)-O(1)**	2.254(4)
O(1)-Ni(1)-N(1)	92.88(8)	**O(2)-Ni(1)-O(1)**	170.76(17)
O(2)-Ni(1)-N(1)	94.82(8)	**O(2)-Ni(1)-O(7)**	91.34(16)
O(1)-Ni(1)-O(4)	81.15(6)	**O(1)-Ni(1)-O(7)**	82.10(16)
O(2)-Ni(1)-O(4)	90.99(7)	**O(2)-Ni(1)-N(1)**	92.86(18)
N(1)-Ni(1)-O(4)	173.79(7)	**O(1)-Ni(1)-N(1)**	93.28(18)
O(1)-Ni(1)-N(2)	97.59(9)	**O(7)-Ni(1)-N(1)**	174.32(19)
O(2)-Ni(1)-N(2)	87.76(10)	**O(2)-Ni(1)-N(2)**	89.9(2)
N(1)-Ni(1)-N(2)	85.12(10)	**O(1)-Ni(1)-N(2)**	97.4(2)
O(4)-Ni(1)-N(2)	97.31(8)	**O(7)-Ni(1)-N(2)**	98.0(2)
O(1)-Ni(1)-O(1)#1	80.67(8)	**O(7)-Ni(1)-O(4)**	76.09(16)
O(2)-Ni(1)-O(1)#1	93.40(8)	**N(1)-Ni(1)-O(4)**	99.78(19)
N(1)-Ni(1)-O(1)#1	99.51(9)	**N(2)-Ni(1)-O(4)**	172.89(19)
O(4)-Ni(1)-O(1)#1	77.92(6)	**O(5)-Ni(2)-O(7)**	90.75(19)
N(2)-Ni(1)-O(1)#1	175.11(8)	**O(4)-Ni(2)-O(7)**	82.48(16)
C(1)-O(1)-Ni(1)	125.23(16)	**O(7)-Ni(2)-N(3)**	174.81(19)
C(1)-O(1)-Ni(1)#1	141.64(17)	**O(7)-Ni(2)-N(4)**	97.8(2)
Ni(1)-O(1)-Ni(1)#1	84.03(6)	**Ni(2)-O(7)-Ni(1)**	88.27(15)

Table S2. Atomic coordinates ($\times 10^4$) and equivalent isotropic displacement parameters ($A^2 \times 10^3$) for complex **1**. U(eq) is defined as one third of the trace of the orthogonalized Uij tensor.

	x	y	z	U(eq)
Ni(1)	257(1)	2554(1)	3848(1)	40(1)
O(1)	656(1)	2094(1)	2401(2)	45(1)
O(2)	-250(1)	3100(1)	5073(2)	55(1)
O(3)	-730(1)	4127(2)	3865(2)	71(1)
O(4)	0	3479(2)	2500	44(1)
N(1)	533(1)	1553(2)	5030(2)	51(1)
N(2)	1161(1)	3084(2)	4957(2)	59(1)
C(1)	1084(1)	1477(2)	2522(3)	46(1)
C(2)	1604(2)	1460(2)	1814(3)	57(1)
C(3)	2043(2)	812(2)	1979(3)	67(1)
C(4)	2020(2)	179(2)	2809(3)	64(1)
C(5)	1524(2)	214(2)	3517(3)	57(1)
C(6)	1062(1)	841(2)	3391(3)	48(1)
C(7)	539(2)	826(2)	4208(3)	53(1)
C(8)	1211(2)	1723(2)	5838(3)	72(1)
C(9)	1295(2)	2597(2)	6145(4)	77(1)
C(10)	-613(2)	3718(2)	4879(3)	61(1)
C(11)	-937(3)	3975(3)	5970(4)	101(2)
C(12)	1683(2)	2148(3)	941(4)	82(1)
C(13)	2518(2)	-506(2)	2963(5)	93(1)
C(14)	31(2)	1396(2)	5833(3)	77(1)
C(15)	1716(2)	3074(3)	4271(4)	92(1)
C(16)	1078(2)	3926(2)	5338(5)	97(1)

Table S3. Anisotropic displacement parameters ($A^2 \times 10^3$) for complex **1**. The anisotropic displacement factor exponent takes the form: $-2\ pi^2\ [\ h^2\ a^{*2}\ U11 + ... + 2\ h\ k\ a^*\ b^*\ U12]$

	U11	U22	U33	U23	U13	U12
Ni(1)	41(1)	36(1)	42(1)	1(1)	9(1)	2(1)
O(1)	43(1)	43(1)	50(1)	6(1)	15(1)	8(1)
O(2)	67(1)	47(1)	53(1)	-2(1)	18(1)	12(1)
O(3)	87(2)	64(2)	67(1)	6(1)	24(1)	31(1)
O(4)	48(2)	34(1)	46(1)	0	4(1)	0
N(1)	63(2)	45(1)	45(1)	4(1)	12(1)	6(1)
N(2)	56(2)	51(2)	65(2)	3(1)	-3(1)	-7(1)
C(1)	37(2)	46(2)	55(2)	-4(1)	12(1)	4(1)
C(2)	45(2)	66(2)	63(2)	-7(2)	20(1)	2(2)
C(3)	38(2)	83(3)	80(2)	-24(2)	14(2)	8(2)
C(4)	44(2)	56(2)	86(2)	-24(2)	-1(2)	12(2)
C(5)	53(2)	42(2)	71(2)	-6(1)	1(1)	10(1)
C(6)	44(2)	43(2)	55(2)	-2(1)	7(1)	6(1)
C(7)	63(2)	36(2)	59(2)	9(1)	17(1)	4(1)
C(8)	88(3)	64(2)	51(2)	5(2)	-14(2)	14(2)
C(9)	78(3)	77(3)	62(2)	-1(2)	-14(2)	4(2)
C(10)	73(2)	54(2)	60(2)	-6(2)	22(2)	12(2)
C(11)	152(4)	88(3)	77(2)	1(2)	54(3)	50(3)
C(12)	63(2)	99(3)	98(3)	14(2)	45(2)	5(2)
C(13)	58(2)	72(3)	140(3)	-33(3)	1(2)	26(2)
C(14)	120(3)	55(2)	71(2)	16(2)	55(2)	11(2)
C(15)	51(2)	123(4)	96(3)	-12(3)	5(2)	-31(2)
C(16)	90(3)	60(3)	124(3)	-28(2)	-13(2)	-15(2)

Table S4. Hydrogen coordinates ($\times 10^4$) and isotropic displacement parameters ($A^2 \times 10^3$) for complex **1**.

	x	y	z	U(eq)
H(3)	2374	803	1499	80
H(5)	1498	-196	4098	69
H(7A)	99	767	3642	63
H(7B)	616	359	4765	63
H(8A)	1551	1553	5382	87
H(8B)	1273	1420	6636	87
H(9A)	990	2753	6686	92
H(9B)	1750	2695	6624	92
H(11A)	-601	4196	6659	152
H(11B)	-1141	3520	6283	152
H(11C)	-1274	4372	5661	152
H(12A)	2119	2123	735	124
H(12B)	1639	2645	1371	124
H(12C)	1343	2116	159	124
H(13A)	2967	-295	3115	140
H(13B)	2434	-823	2189	140
H(13C)	2470	-834	3681	140
H(14A)	167	937	6371	115
H(14B)	-400	1295	5279	115
H(14C)	2	1854	6365	115

H(15A)	2110	3305	4811	138
H(15B)	1591	3379	3487	138
H(15C)	1809	2531	4066	138
H(16A)	710	3961	5766	145
H(16B)	989	4259	4582	145
H(16C)	1483	4104	5914	145

Table S5. Atomic coordinates ($\times 10^4$) and equivalent isotropic displacement parameters ($A^2 \times 10^3$) for complex **2**. U(eq) is defined as one third of the trace of the orthogonalized Uij tensor.

	x	y	z	U(eq)
Ni(1)	8550(1)	6641(1)	7500(1)	34(1)
Ni(2)	6847(1)	5859(1)	7633(1)	38(1)
Cl(1)	7750(2)	3530(1)	6873(1)	61(1)
Cl(2)	7880(2)	3985(1)	3822(1)	62(1)
Cl(3)	6996(2)	9019(1)	7264(1)	62(1)
Cl(4)	3614(2)	8896(2)	4388(1)	70(1)
O(1)	7793(3)	5505(3)	6939(2)	38(1)
O(2)	9117(3)	7790(3)	8114(3)	43(1)
O(3)	8753(4)	7700(3)	9243(3)	60(1)
O(4)	6929(3)	7052(3)	7123(3)	40(1)
O(5)	6985(4)	4651(3)	8172(3)	53(1)
O(6)	8587(5)	4668(4)	9091(4)	81(2)
O(7)	8254(3)	6201(3)	8510(2)	41(1)
N(1)	8709(4)	7032(3)	6406(3)	39(1)
N(2)	10023(4)	6115(4)	7925(3)	47(1)
N(3)	5460(4)	5562(4)	6663(3)	44(1)
N(4)	6038(5)	6321(4)	8339(4)	55(2)

C(1)	7750(4)	5170(4)	6225(4)	36(1)
C(2)	7735(5)	4247(4)	6079(4)	43(1)
C(3)	7741(5)	3878(4)	5345(4)	46(2)
C(4)	7778(5)	4424(4)	4715(4)	44(1)
C(5)	7776(4)	5344(4)	4813(4)	41(1)
C(6)	7777(4)	5709(4)	5555(4)	36(1)
C(7)	7826(5)	6707(4)	5643(4)	37(1)
C(8)	8739(7)	8005(5)	6329(5)	59(2)
C(9)	9655(5)	6632(5)	6458(4)	50(2)
C(10)	10404(5)	6614(5)	7390(5)	55(2)
C(11)	10054(6)	5145(5)	7807(6)	66(2)
C(12)	10651(6)	6309(7)	8840(5)	70(2)
C(13)	9115(5)	8092(4)	8800(4)	42(1)
C(14)	9598(6)	8985(5)	9084(5)	56(2)
C(15)	6177(4)	7465(4)	6509(4)	38(1)
C(16)	6096(5)	8384(4)	6463(4)	41(1)
C(17)	5331(5)	8838(5)	5825(4)	46(2)
C(18)	4587(5)	8352(5)	5209(4)	47(2)
C(19)	4609(5)	7434(5)	5229(4)	45(1)
C(20)	5381(5)	6978(4)	5869(4)	40(1)
C(21)	5360(5)	5992(5)	5859(4)	46(2)
C(22)	5318(6)	4582(5)	6499(5)	61(2)
C(23)	4703(5)	5904(6)	6942(5)	58(2)
C(24)	5079(6)	5826(6)	7900(5)	60(2)
C(25)	5883(7)	7284(6)	8310(6)	70(2)
C(26)	6531(7)	6038(6)	9252(5)	67(2)
C(27)	7756(7)	4295(5)	8710(5)	61(2)
C(28)	7665(10)	3335(6)	8924(6)	93(3)

Table S6. Anisotropic displacement parameters ($A^2 \times 10^3$) for complex **2**. The anisotropic displacement factor exponent takes the form $-2\,pi^2\,[\,h^2\,a^{*2}\,U11 + ... + 2\,h\,k\,a^*\,b^*\,U12\,]$

	U11	U22	U33	U23	U13	U12
Ni(1)	38(1)	34(1)	31(1)	-3(1)	16(1)	-4(1)
Ni(2)	40(1)	39(1)	36(1)	-1(1)	17(1)	-8(1)
Cl(1)	81(1)	39(1)	68(1)	7(1)	37(1)	2(1)
Cl(2)	69(1)	65(1)	60(1)	-27(1)	34(1)	-4(1)
Cl(3)	66(1)	42(1)	61(1)	-10(1)	11(1)	-2(1)
Cl(4)	52(1)	77(1)	67(1)	21(1)	13(1)	14(1)
O(1)	46(2)	32(2)	38(2)	-4(2)	20(2)	-5(2)
O(2)	51(3)	42(2)	40(2)	-13(2)	24(2)	-11(2)
O(3)	87(4)	59(3)	50(3)	-14(2)	43(3)	-21(3)
O(4)	38(2)	41(2)	39(2)	-3(2)	16(2)	-4(2)
O(5)	65(3)	47(3)	45(2)	4(2)	22(2)	-12(2)
O(6)	81(4)	61(4)	69(4)	21(3)	2(3)	-10(3)
O(7)	46(2)	44(2)	33(2)	0(2)	15(2)	-9(2)
N(1)	55(3)	34(3)	37(2)	-6(2)	27(2)	-6(2)
N(2)	45(3)	51(3)	44(3)	0(2)	19(2)	2(2)
N(3)	42(3)	44(3)	45(3)	-4(2)	18(2)	-9(2)
N(4)	56(4)	70(4)	48(3)	-5(3)	30(3)	-14(3)
C(1)	33(3)	35(3)	38(3)	-8(2)	13(2)	-2(2)
C(2)	40(3)	36(3)	52(3)	-7(3)	19(3)	-3(3)
C(3)	44(4)	39(3)	56(4)	-12(3)	21(3)	-1(3)
C(4)	38(3)	49(4)	46(3)	-16(3)	18(3)	-3(3)
C(5)	37(3)	44(3)	40(3)	-10(3)	16(3)	0(3)
C(6)	37(3)	33(3)	36(3)	-1(2)	14(2)	1(2)
C(7)	49(3)	33(3)	33(3)	-1(2)	19(3)	3(3)
C(8)	94(6)	40(4)	49(4)	-3(3)	37(4)	-17(4)
C(9)	45(4)	64(4)	50(4)	-5(3)	28(3)	-6(3)

C(10)	41(4)	65(5)	60(4)	-10(4)	22(3)	-10(3)
C(11)	56(5)	52(4)	87(6)	4(4)	28(4)	13(4)
C(12)	45(4)	96(7)	55(4)	-4(4)	6(3)	12(4)
C(13)	39(3)	45(3)	41(3)	-10(3)	18(3)	-5(3)
C(14)	61(4)	58(4)	55(4)	-26(3)	30(3)	-21(3)
C(15)	37(3)	46(3)	34(3)	-4(2)	18(2)	-2(3)
C(16)	43(3)	39(3)	44(3)	-4(3)	20(3)	0(3)
C(17)	49(4)	46(4)	47(3)	2(3)	25(3)	5(3)
C(18)	38(3)	56(4)	46(3)	10(3)	17(3)	6(3)
C(19)	36(3)	55(4)	40(3)	-1(3)	13(3)	-2(3)
C(20)	38(3)	43(3)	40(3)	-3(3)	18(3)	-1(3)
C(21)	45(4)	48(4)	40(3)	-5(3)	12(3)	-5(3)
C(22)	66(5)	45(4)	60(4)	-12(3)	15(4)	-17(3)
C(23)	42(4)	72(5)	65(4)	-11(4)	27(3)	-8(3)
C(24)	54(4)	71(5)	63(4)	5(4)	34(4)	-14(4)
C(25)	90(6)	68(5)	73(5)	-11(4)	53(5)	-3(5)
C(26)	85(6)	86(6)	40(4)	-5(4)	36(4)	-10(5)
C(27)	86(6)	47(4)	44(4)	8(3)	21(4)	-6(4)
C(28)	133(9)	60(5)	69(6)	22(4)	25(6)	-8(6)

Table S7. Hydrogen coordinates ($\times 10^4$) and isotropic displacement parameters ($A^2 \times 10^3$) for complex **2**.

	x	y	z	U(eq)
H(3)	7720	3252	5275	55
H(5)	7774	5722	4372	49
H(7A)	7841	6968	5122	45
H(7B)	7213	6920	5682	45
H(8A)	8798	8157	5799	88
H(8B)	9313	8242	6819	88

H(8C)	8126	8263	6317	88
H(9A)	9920	6987	6116	60
H(9B)	9530	6022	6224	60
H(10A)	11030	6338	7433	66
H(10B)	10557	7230	7605	66
H(11A)	9705	5001	7197	99
H(11B)	9728	4842	8123	99
H(11C)	10748	4950	8021	99
H(12A)	11343	6147	8978	106
H(12B)	10411	5966	9198	106
H(12C)	10615	6944	8947	106
H(14A)	10257	8984	9078	83
H(14B)	9668	9109	9665	83
H(14C)	9183	9444	8694	83
H(17)	5320	9468	5812	55
H(19)	4088	7111	4798	54
H(21A)	4724	5797	5394	56
H(21B)	5905	5777	5718	56
H(22A)	5394	4278	7025	92
H(22B)	5817	4359	6313	92
H(22C)	4650	4470	6051	92
H(23A)	4078	5562	6660	70
H(23B)	4557	6534	6771	70
H(24A)	4576	6068	8081	72
H(24B)	5184	5193	8067	72
H(25A)	5503	7438	8639	105
H(25B)	5514	7473	7715	105
H(25C)	6530	7585	8557	105
H(26A)	7234	6214	9494	101
H(26B)	6483	5393	9287	101
H(26C)	6201	6322	9575	101
H(28A)	8322	3052	9143	140
H(28B)	7210	3024	8407	140
H(28C)	7404	3306	9360	140

Section S7. References

References

1. Kundu, B. K.; Ranjan, R.; Mukherjee, A.; Mobin, S. M.; Mukhopadhyay, S., Mannich base Cu(II) complexes as biomimetic oxidative catalyst. *J. Inorg. Biochem.* **2019,** *195*, 164-173.
2. *SAINT V8.34A; Bruker AXS Inc.* **2013**.
3. *SHELXTL -2014/7; Bruker AXS Inc.* **2014**.
4. (a) McKinnon, J. J.; Jayatilaka, D.; Spackman, M. A., Towards quantitative analysis of intermolecular interactions with Hirshfeld surfaces. *Chem. Commun.* **2007,** (37), 3814-3816; (b) Spackman, M. A.; McKinnon, J., Fingerprinting intermolecular interactions in molecular crystals. *CrystEngComm* **2002,** *4* (66), 378-392.
5. Spackman, M. A.; Byrom, P. G., A novel definition of a molecule in a crystal. *Chem. Phys. Lett.* **1997,** *267* (3-4), 215-220.
6. McKinnon, J. J.; Spackman, M. A.; Mitchell, A. S., Novel tools for visualizing and exploring intermolecular interactions in molecular crystals. *Acta Crystallogr. Sect. B: Struct. Sci.* **2004,** *60* (6), 627-668.
7. Rohl, A. L.; Moret, M.; Kaminsky, W.; Claborn, K.; McKinnon, J. J.; Kahr, B., Hirshfeld Surfaces Identify Inadequacies in Computations of Intermolecular Interactions in Crystals: Pentamorphic 1,8-Dihydroxyanthraquinone. *Crystal Growth & Design* **2008,** *8* (12), 4517-4525.
8. Wolff, S.; Grimwood, D.; McKinnon, J.; Turner, M.; Jayatilaka, D.; Spackman, M., Crystal explorer. University of Western Australia Crawley, Australia: 2012.
9. Kundu, B. K.; Pragti; Mobin, S. M.; Mukhopadhyay, S., Studies on the influence of the nuclearity of zinc(II) hemi-salen complexes on some pivotal biological applications. *Dalton Transactions* **2020,** *49* (43), 15481-15503.
10. Bolleter, W. T.; Bushman, C. J.; Tidwell, P. W., Spectrophotometric Determination of Ammonia as Indophenol. *Anal. Chem.* **1961,** *33* (4), 592-594.
11. Kundu, B. K.; Pragti; Mukhopadhyay, S., Synthesis of Aminocyanopyridines Using Urease Mimetics, **2021,** *Patent Filled: Application No. TEMP/E-1/4288/2021-KOL, Ref. No. 202131004379, CBR No. 2179.*
12. (a) Bag, B.; Mondal, N.; Rosair, G.; Mitra, S., The first thermally-stable singly oxo-bridged dinuclear Ni (III) complex. *Chem. Commun.* **2000,** (18), 1729-1730; (b) Kundu, B. K.; Mandal, P.; Mukhopadhyay, B. G.; Tiwari, R.; Nayak, D.; Ganguly, R.; Mukhopadhyay, S., Substituent dependent sensing behavior of Schiff base chemosensors in detecting Zn^{2+} and Al^{3+} ions: Drug sample analysis and living cell imaging. *Sensors and Actuators B: Chemical* **2019,** *282*, 347-358.